# Structural Design of Acryl/Silica Nano-Composite Emulsions and Their Films

**Koji Arai**

**Kyoto Institute of Technology**

**2019**

## Contents

# General Introduction

## Organic/inorganic hybrid materials

Various materials existing around us are generally composed of organic and inorganic substances. These two classes of substances have been studied separately to contribute to the development of materials. Recently, a technology has been developed to create organic/inorganic hybrid materials in which both organic and inorganic substances are combined. For instance, organic polymers are strengthened by incorporating several types of inorganic fillers. The organic polymers are characterized by light weight, flexibility, and high impact resistance as well as excellent processability, although they are inferior to inorganic materials in strength and heat resistance. On the other hand, the inorganic materials such as glass and ceramics show excellent durability and heat resistance, although they are inferior to organic substances owing to their heavier weight, weaker impact strength, and higher manufacturing cost. The organic/inorganic hybrid materials, in return, exhibit the advantageous properties of both components and improve the disadvantageous properties of each component to lead the development of various high-performance and highly functional materials.

An active research on such organic-inorganic hybrid materials has been conducted in the 1980s mainly for the purpose of reducing the weight of automobiles. In the 1990s, many studies were done for hybridizing organic polymers with inorganic nanoparticles whose diameter is in the order of nanometer (nm). Such materials were called organic/inorganic nanocomposites and have been attracting much attention until now because they show dramatically improved performance by incorporating a small amount of inorganic nanoparticles into their matrix polymers.

**Organic/inorganic nanocomposite materials**

The properties of the organic/inorganic nanocomposites (simply referred to as nanocomposites) are greatly influenced by the dispersion state of inorganic nanoparticles in the matrix polymers, which is, of course, strongly influenced by the surface characteristics of the nanoparticles. Preparation of nanocomposite materials are often carried out by high shear stirring or simple mixing with a ball mill, but the dispersed inorganic nanoparticles are likely to aggregate during the mixing to form an inhomogeneous mixing state with minimal nanosize effects of the nanoparticles included [1]. The most reliable method for better dispersion of the inorganic nanoparticles is to coat the inorganic particles with a matrix polymer itself to form a hybrid core/shell structure, and by which the inorganic nanoparticles are placed in the organic matrix polymer without aggregation. Therefore, many researchers have actively studied on the synthesis of such hybrid core/ shell nanoparticles until now [2]. At present, several core/ shell nanoparticles are proposed as building blocks in preparing hybrid films with intriguing physicochemical properties, which are originated from specific interfacial interactions between the inorganic nanoparticles and matrix polymer [3,4]. One of the most convenient methods for incorporating nanoparticles into a polymer matrix is to use miniemulsion polymerization. In this method, monomer droplets of c.a. 50 to 500 nm in diameter suitably incorporate the nanoparticles and achieve encapsulation by subsequent polymerization. Landfester [5], Wu et al. [6], and Cao et al. [7] separately reviewed various miniemulsion processes for synthesizing such hybrid nanoparticles. In order to efficiently incorporate nanoparticles into the organic polymer matrix, the compatibility of the inorganic particles with the organic monomer must be improved by surface modification of the inorganic particles [8]. In the case of silica nanoparticles, the modification can be

accomplished by surface reaction with such organic silane coupling agents [9-14]. The resultant silica nanoparticles having modified surface can efficiently be distributed to the acrylic monomer phase and encapsulated by the subsequent polymerization [15]. Such surface modification is also possible by simple adsorption of cationic surfactants [16,17] or cationic initiators [18] on the anionically charged silica surface. In the latter case, the polymerization is initiated from the adsorption sites to generate a polymer layer on the silica surface. Addition of cationic monomers such as 4-vinylpyridine has also been shown effective for polymerization on silica surface [19]. Furthermore, aliphatic carboxylic acids such as oleic acid are also known to work as surface modifiers of colloidal silica particles [8,20,21]. Even in living/controlled radical polymerization (L/CRP) such as reversible addition-fragmentation chain transfer (RAFT) polymerization [22-24] and atom transfer radical polymerization [25] in water dispersion system can be conducted for obtaining hybrid nanoparticles coated with polymers with controlled molecular weight and molecular weight distribution. Raspberry-type hybrid nanoparticles are also prepared by Pickering-type miniemulsion polymerization [26] as well as by competitive polymerization of vinyl monomers and inorganic precursors [27]. In these emulsion systems, however, control of the encapsulation of the inorganic particles is not so easy, making the emulsion stability unfavorably lower [28]. As Bourgeat-Lami et al. reported [28], the inorganic particle distribution in the resultant miniemulsion is not homogeneous even when the surface-modified nanoparticles are dispersed in acrylic monomer phase. Namely, it has been confirmed that the obtained emulsion contains hybrid particles having polymer particles lacking core inorganic nanoparticles and a plurality of inorganic particles in the core [29]. In addition, the emulsification of mini-emulsion droplets containing nanoparticles requires highly effective sonication and high-pressure homogenizers [30], so the mini-emulsion polymerization

method may not readily be utilized in large-scale industrial production of hybrid particles [31].

**Nano-composite emulsion (NCE)**

Previously, the author et al. succeeded in obtaining colloidal silica/polyacrylate hybrid particles by the ordinary emulsion polymerization method with the aid of a nonionic surfactant showing a lower critical solution temperature (LCST) or cloud point ($T_{cp}$). In this method (Scheme 1), each of the colloidal silica particles of 20~50 nm in diameter was successfully covered with a polyacrylate coat of ca. 15~20 nm in thickness in a core/shell form. With this feature, the resultant emulsion was called "nano-composite emulsion (NCE)" [32, 33]. Later, another group also traced the same method to obtain NCE [34].

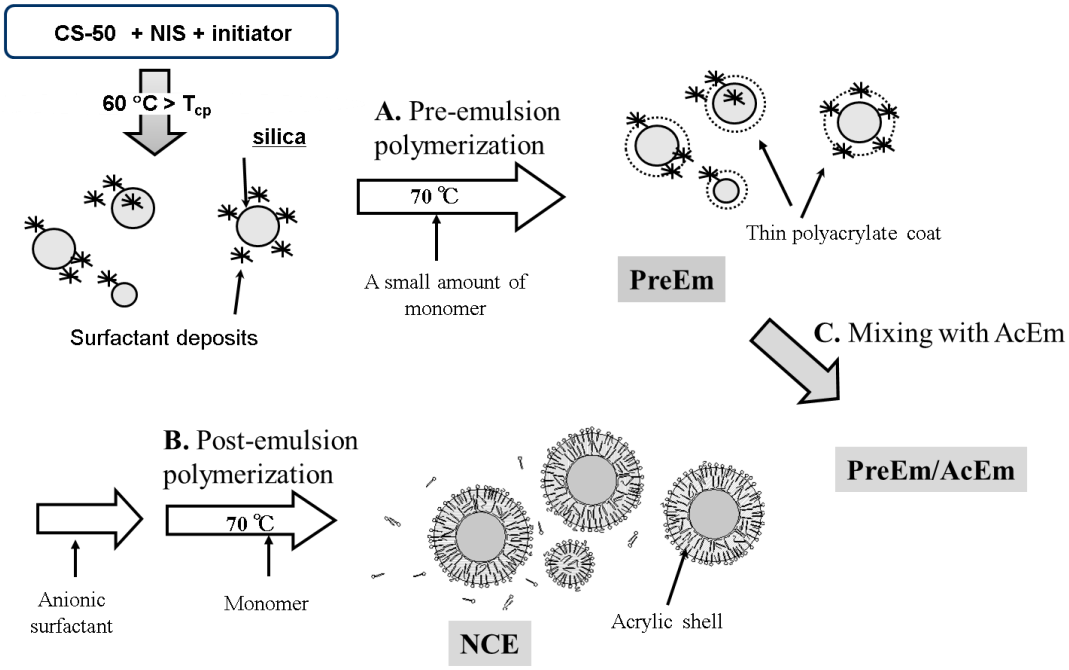


**Scheme 1. Synthetic routes to NCE (steps A and B) and hybrid emulsions (steps A and C)**

In our practical procedure (steps (A) and (B) in Scheme 1), an aqueous dispersion of silica nanoparticles (CS-50) was mixed with such a nonionic surfactant (NIS) and warmed up above its $T_{cp}$ with stirring to make the surfactant deposit on the surface of the colloidal silica particles. Then, a small amount of monomer was adsorbed on the surface of the surfactant-deposited particles and polymerized to form a thin organic layer. After this pre-emulsion polymerization (step A), the post-emulsion polymerization (step B) was continued to obtain the NCE, which could readily form highly transparent hybrid films by casting even at a silica content above 50 wt.%. This NCE process is simple as a polymerization method in contrast to the mini-emulsion process, and its industrial application is possible. The hybrid film obtained from NCE exhibited various interesting properties such as antifouling property and fire resistance that are essential for use as high quality wall paints [32,33,35].

**About this study**

As described above, the organic/inorganic nanocomposite materials are of growing interest because they combine the advantages of both matrix polymers and nanoparticle fillers. They are highly useful in a wide range of industrial applications in such fields as cosmetics, plastics, rubbers, inks and coatings. However, the control of dispersion state of nanoparticles in the matrix polymer is not easily accomplished to attain maximum properties. In NCE, developed by the author's research group, the core/shell hybrid structure of emulsion particles can readily established to afford hybrid films having a well-dispersed state of silica nanoparticles by the simple casting method. So in Chapter 1, transparent films were prepared from a number of NCEs having different compositions, and the mechanical and thermal properties of the films were compared to those of films prepared by simple blending of acrylic

emulsions with silica sol.

On the other hand, the recipe for preparing NCE is rather complex compared to the ordinary emulsion polymerization, and the NCEs sometimes cause gelation during the post-emulsion polymerization or the paint formulation. Thus, a simpler recipe for manipulating silica nanoparticles is required to prepare water-borne hybrid emulsions. Therefore, the author decided to reinvestigate the structural changes of the colloidal particles formed in each step of preparation of NCE for the purpose of inventing a simpler method. Chapter 2 deals with such a different process in using NCEs. At first was highlighted the first step of pre-emulsion polymerization in which the nonionic surfactant with lower $T_{cp}$ is allowed to effectively deposit on the surface of colloidal silica particles by the clouding behavior and aid acrylic monomers to settle around the silica particles and generate a thin polymer coat on the particle surface by the subsequent polymerization. This feature indicated that the resultant colloidal silica particles are covered with a thin polyacrylate coat, being stabilized or hard in aggregation. These NCEs having a thin polyacrylate coat were called PreEms. Here, the PreEms have been shown to function as effective inorganic modifiers for common acrylic emulsions, giving hybrid films with interesting properties.

This thesis comprises two chapters dealing with the different NCEs in addition to the present General Introduction. The abstracts of the two chapters are as follows.

**Chapter 1. Unique structure and properties of inorganic-organic hybrid films prepared from acryl/ silica nano-composite emulsions.**

Transparent films were prepared from nano-composite emulsions, which contained

nano-size core-shell-type particles (ca. 60 nm in diameter) consisting of colloidal silica (inorganic core, ca. 30 nm in diameter) and poly(methyl methacrylate-*co*-*n*-butyl acrylate) (organic shell). The silica content in the film could be increased up to 150 wt/wt% by keeping its homogeneity. It was revealed that the formation of such a core-shell structure is guided by the surface sedimentation of a nonionic surfactant above its clouding point to form an organic thin layer that can provide the sites for monomer absorption and polymerization. The thermal and mechanical properties of the resultant nano-composite films were evaluated by various methods and compared with those of simple blend films of the corresponding acrylic emulsion and colloidal silica. It was clarified that the high-temperature strength of the nano-composite films can be improved by the reinforcement effect of silica particles.

**Chapter 2. Colloidal silica bearing thin polyacrylate coat: A facile inorganic modifier of acrylic emulsions for fabricating hybrid films with least aggregation of silica nanoparticles.**

Novel nano-composite emulsions consisting of colloidal silica particles covered with thin polyacrylate coat (PreEm) were successfully prepared with the aid of a nonionic surfactant having a low cloud point ($T_{cp}$ = 40 °C). This nonionic surfactant first deposited on the surface of colloidal silica particles above its $T_{cp}$ to provide the sites for adsorption and the following polymerization of acrylic monomer. Scanning transmission electron microscopy of the colloidal particles obtained after the polymerization indicated the presence of very thin coat layer of polyacrylate (c.a., 1 - 3 nm in thickness) around silica nanoparticles. These PreEm particles were readily incorporated into the ordinary acrylic

emulsions (AcEm) to obtain silica/ polyacrylate mixed emulsions (PreEm/ AcEm). It was revealed that the mixed emulsions can give transparent coating films at a silica/polyacrylate ratio below 150/100 in which the colloidal particles were distributed in the polymer matrix without aggregation. This morphology was in sharp contrast with the particle aggregation morphologies shown by the films obtained from the naked colloidal silica-AcEm mixed emulsion and the conventional nanocomposite emulsion consisting of silica particles covered with thick polyacrylate coat. The PreEm/ AcEm films exhibited increased hardness with increasing the silica contents to 150 %. These data supported the effectiveness of PreEm in controlling the properties of silica-polyacrylate hybrid films.

## References


1. M. Xiong, L. Wu, S. Zhou, B. You, *Polym. Int.*, **51**, 693 (2002).
2. M. Jianzhong, B. Yan, Z. Jing, *Adv, colloid and Interface Sci*., **197-198,** 118 (2013).
3. N. Dechao, Li. Yongsheng, S. Jianlin, *Chemical Society Reviews*, **46**, 569 (2017).
4. R. Tania, B. Carlos, F. Jose Paulo S., *Materials*, **7**, 3881 (2014).
5. K. Landfester, Angew. *Chem. Int. Ed.,* **48**, 4488 (2009).
6. J. Hu, M. Chen, L. Wu, *Polym. Chem.,* **2**, 760 (2011).
7. D. Qi, Z. Cao, U. Ziener, *Adv. Colloid Interf. Sci.*, **211**, 47 (2014).
8. M. Hood, M. Mari, R. Muñoz-Espí, *Materials*, **7**, 4057 (2014).
9. E. Bourgeat-Lami, J. Lang, *J. Coll. Int. Sci.,* **210**, 281 (1999).
10. R. Hashemi-Nasab, SM. Mirabedini, *Prog. Org. Coat.,* **76**, 1016 (2013).
11. S. Song, S. Sun, H. Zhang, *Journal of Polymer Research,* **23**, 119 (2016).
12. ZB. Zhao, L. Tai, DM. Zhang, ZF. Wang, Y. Jiang, *Chem. Eng. J.,* **307**, 891 (2017).
13. H. Li, J. Yuan, H. Qian, L. Wu, *Prog. Org. Coat.,* **97**, 65-73 (2016).
14. Y. Wu, D. Hu, YH. Su, YL. Hsiao, B. You, L. Wu, *Prog. Org. Coat.,* **77** (6), 1015 (2014).
15. LL. Hecht, C. Wagner, Ö. Özcan, F .Eisenbart, K .Köhler, K .Landfester, HP. Schuchmann, Macromol. *Chem. Phys.*, **213**, 2165 (2013).
16. G. Canché-Escamilla, S. Duarte-Aranda, M. Toledano, Mat. Sci. Eng. C., **42**, 161 (2014).
17. I. Sondi, TH. Fedynyshyn, R. Sinta, E. Matijevic, *Langmuir,* **16**, 9031 (2000).
18. MJ. Percy, SP. Armes, *Langmuir,* **18**, 4562 (2002).
19. MJ. Percy, C. Barthet, JC. Lobb, MA. Khan, SF. Lascelles, M. Vamvakaki. SP. Armes *Langmuir,* **16**, 6913 (2000).

20. M. Khalina, M. Sanei, HS. Mobarakeh, AR. Mahdavian, *Int. J. Adhes. Adhes.*, **58**, 21 (2015).

21. J. Ji, S. Shu, F. Wang, J. Liu, ZZ. Yu, *Colloid. Surf. A: Physicochem. Eng. Asp.*, **446**, 156 (2014).

22. D. Tumnantong, GL. Rempel, P. Prasassarakich, *European Polymer Journal*, **80**, 145 (2016).

23. E. Bourgeat-Lami, AJPG. França, TC. Chaparro, RD. Silva, PY. Dugas, GM. Alves, AM. Santos, *Macromolecules*, **49,** 4431 (2016).

24. XG. Qiao, O. Lambert, JC. Taveau, PY. Dugas, B. Charleux, M. Lansalot, E. Bourgeat-Lami, *Macromolecules*, **50**, 3796 (2017).

25. A. Khabibullin, E. Mastan, K. Matyjaszewski, S. Zhu, *Controlled Radical Polymerization at and from Solid Surfaces*, 29 (2015).

26. J. Ji, S. Shu, F. Wang, Z. Li, J. Liu, Y. Song, Y. Jia, *Nanoscale research letters*, **9**, 534 (2014)

27. X. Zhou, H. Shao, H. *Liu*, *Coll. Polym. Sci.*, **291**, 1181 (2013)

28. E. Bourgeat-Lami, GA. Farzi, L. David, JL. Putaux, TFL. McKenna, *Langmuir,* **28**, 6021 (2012).

29. K. Hamada, M. Kohri, T. Taniguchi, K. Kishikawa, *Colloid. Surf. A: Physicochem. Eng. Asp.*, **512**, 81 (2017).

30. LL. Hecht, T. Merkel, A. Schoth, C. Wagner, K. Köhler, R. Muñoz-Espí, K. Landfester, HP. Schuchmann, *Chem. Eng. J.*, **229**, 206 (2013).

31. LL. Hecht, T. Merkel, A. Schoth, C. Wagner, K. Köhler, R. Muñoz-Espí, *Chem. Eng. J.* **229**, 206 (2013).

32. T. Mizutani, K. Arai, M. Miyamoto, Y. Kimura, *J. Appl. Polym. Sci.*, **99**, 659 (2006).

33. T. Mizutani, K. Arai, M. Miyamoto, Y. Kimura, *Prog. Org. Coat.*, **55**, 276 (2006).

34. M. Yazdimamaghani, T. Pourvala, E. Motamedi, B. Fathi, D. Vashaee, L. Tayebi, *Materials*, **6**, 3727 (2013).

35. K. Arai, T. Mizutani, Y. Kimura, M. Miyamoto, *Prog. Org. Coat.*, **93,** 109 (2016).

## Abbreviation

NCE, Nano-composite emulsion.

PreEm, Colloidal particles in pre-emulsion state or surface-coated colloidal silica particles.

AcEm, The ordinary acrylic emulsion.

CS-50, Colloidal silica with 50wt% silica content.

NIS, Nonionic surfactant: Poly(ethylene glycol) mono- [1-(allyloxy)-3-(4-nonylphenoxy) -2-propyl] ether.

LCST; Lower critical solution temperature.

Tcp, Cloud point.

Tg, Glass transition temperature.

SDS, Sodium dodecylbenzenesulfonate.

APS, Ammonium persulfate.

KPS, Potassium persulfate.

n-BA, Butyl acrylate.

MMA, Methyl methacrylate.

MAA, Methacrylic acid.

DLS, Dynamic light scattering.

STEM, Scanning transmission electron microscopy.

SEM, Scanning electron microscopy.

AFM, Atomic force microscopy.

FT-IR, Fourier transform infrared spectrometry.

DMA, Dynamic mechanical analysis.

TGA, Thermogravimetric analysis.

# Chapter 1

# Unique structure and properties of inorganic-organic hybrid films prepared from acryl/ silica nano-composite emulsions

# INTRODUCTION

In the past decades, many research papers have been published on a variety of nano-composite systems consisting of polymeric materials and inorganic nano-particles. These composite systems are characterized by the unique properties originating from the nano-dispersion state of the inorganic components in the polymer matrix in which the polymer matrix provides excellent processability and flexibility while the inorganic nano-particles provide high mechanical properties and thermal stability [1-19]. These nanocomposite materials usually exhibit much better properties than the conventional organic/inorganic composites having micro- and macro-size structures and can be used for various purposes including plastics, rubbers, fibers, adhesives, and coatings [20-26].

The ordinary nano-particle composites can be obtained by simply mixing inorganic particles in polymeric matrices. However, the nano-particles dispersed likely agglomerate to form an inhomogeneous mixing state with which the nano-size effect of the particles is minimized. In order to achieve the well dispersed state of nano-particles, core/shell-type structure where the inorganic particles are embedded into polymer particles ought to be effective. With this structure, the inorganic particles are separated from each other even when the core/shell-type particles are allowed to aggregate, and the interfacial adhesion between the polymer matrix and the inorganic particles can be retained in maximum. It has been uneasy, however, to encapsulate such nano-particles with polymeric materials. Various physicochemical and chemical processes have ever been tried for such purposes thus far. For instance, polymers are physicochemically precipitated or adsorbed onto the surface of inorganic particles by solvent evaporation or by means of electrostatic force or chemical or biochemical techniques [3-8]. More often, polymerization is performed in the presence of inorganic particles for their coating or inclusion [8-17]. In this case the surface of the

inorganic nano-sized particles ought to be modified in order to make it compatibilize with the organic interface and to prevent the particles from agglomerating during the polymerization. In many cases, the modifiers are covalently bonded onto the surface of inorganic particles prior to the polymerization. For example, the silica particles are pre-treated with an acrylic siloxane coupling agent for producing nano-composite emulsion consisting of nano-scale silica (up to 33 wt%) and poly(ethyl acrylate) (PEA) [8-10]. Alternatively, some surfactants and amphiphilic block copolymers such as urethane-acrylate nonionomers were used for surface modification of the particles [13-16]. They are usually adsorbed on the surface of the particles to afford a monomer-absorbing layer on surface.

Previously [27], the author's research group succeeded in preparing a core/shell-type nano-composite emulsion (NCEs) by using a simple emulsion polymerization technique. In the resultant NCE, each of the nano-scaled particles consisted of a silica nano-particle core of 20~30 nm in diameter and a polyacrylate coating layer having a thickness of ca. 15~20 nm. This nano-scaled encapsulation of silica nano-particles was possible in the presence of nonionic surfactants of low cloud point as the modifiers. Mixing of such a nonionic surfactant in an aqueous dispersion of silica particles allowed the surfactant to precipitate on the surface of the particles above its cloud point to form an organic thin layer that can provide the sites for monomer adsorption and polymerization by which the stable NCEs having a silica-to-polyacrylate ratio up to 150/100 in wt/wt% could readily be prepared. The NCE thus obtained could form stable coating films on various substrates to show various interesting properties.

It has been well known that when inorganic particles are uniformly dispersed in a polymer matrix various improved properties involving mechanical and thermal properties can be attained [7]. With our NCE, silica particles can be dispersed more uniformly in the polymer matrix than with the ordinary blends of colloidal silica and polymer emulsion, and various

interesting properties specific to the nano-dispersed structure are expected to be realized. In fact, the primary distinction of the NCE was in the appearance of the hybrid film because its transparency could be retained at high silica contents. This feature is very important not only for their application to optical materials [25], but also to paint and ink for which color matching is necessary. In this study, therefore, we evaluate various properties of the inorganic-organic hybrid films prepared from acryl/ silica NCEs in relation to the nano-dispersed structure.

## EXPERIMENTAL

### Materials

The colloidal silica used in the present study was ADEKA Corporation ADELITE® AT-50 (abbreviated as CS-50) for which the average diameter of the silica particles was reportedly 20-30 nm and the silica content was 50 wt%. A nonionic surfactant, ADEKA REASOAP® NE-10 (abbreviated as NIS), was used as the reactive nonionic surfactant, which was also the product of ADEKA Corp., Japan. Sodium dodecylbenzenesulfonate (SDS), butyl acrylate (n-BA), methyl methacrylate (MMA), methacrylic acid (MAA), and other chemicals were industrial grade reagents and were used as received.

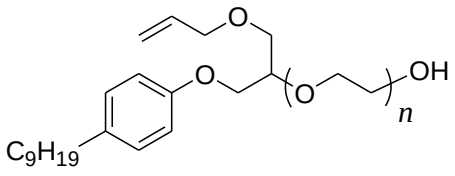


**NIS: n=10**

**Polymerization procedure**

The procedure used for preparing NC1-4 (vide infra) is shown as an example. Prior to the polymerization, a monomer mixture consisting of 69 g of MMA, 130 g of n-BA, and 1.0 g of MAA (or 99.5 g of MMA, 99.5 g of BA, and 1.0 g of MAA for NC2) was prepared. Into a 1 L flask equipped with a condenser, a dropping funnel, and a mechanical stirrer was charged 340 g of CS-50 under nitrogen. A solution of 0.5 g of ammonium persulfate (APS) and 5.0 g of NIS in 140 g of water was added dropwise to CS-50 with vigorous stirring at 60 °C. After the addition, the temperature of the mixture was raised to 70 °C. To this mixture was added dropwise 5 g of the monomer mixture, and the contents were kept at 70 °C for 1 h. Then, a mixture of 0.6 g of APS and 24 g of SDS in 50 g of water and the rest of the monomer mixture were added dropwise sequentially. The reaction mixture was kept at 70°C for an additional hour to complete the polymerization. After the mixture had been cooled to room temperature, 3.6 g of an aqueous ammonia solution (25 wt %) was added to control the emulsion's pH to pH=9-10.

Silica-free emulsions having monomer compositions corresponding to those of NC1-4 were also prepared by the conventional emulsion polymerization. Each of the resultant emulsions was blended with a predetermined amount of colloidal silica CS-50 to prepare the silica-polymer emulsion blends.

**Temperature dependence of a colloidal silica containing NIS**

In an ordinary test tube (A), CS-50 was diluted with distilled water to obtain a colloidal silica of 33.4 wt-% in solid content. In another test tube (B), an aqueous solution of NIS was prepared in a concentration of 5.0 wt-%. In the other test tube (C), a mixed solution of colloidal silica (33.4 wt-%) and NIS (12 wt-%) was prepared. The three tubes were kept at 60 °C for 16 h, cooled down to room temperature overnight, and warmed up again to 60 °C.

The precipitation and gelation feature of each solutions were observed time to time.

**Preparation of nano-composite films**

A certain amount of each of the emulsions was cast on a polyethylene plate or a glass plate (100×150 $mm^2$) with an applicator to prepare a coating film of ca. 100 μm in thickness. The coating film was dried at 50 °C for 16 h to obtain a solid film having a thickness of ca. 40 μm.

**Measurements**

Tensile properties of the films were measured on an Orientec (Tokyo) STA1150 tensiometer. The sample films were cut into a size of 15×50 $mm^2$, and each specimen was stretched at a crosshead speed of 30 mm/min at 25 °C. The tensile properties were automatically calculated by the computer connected to the machine, and the average of at least six measurements was taken for each measurement. Dynamic mechanical analysis (DMA) was performed on a Rheogel-E4000 in tension mode at 32 Hz in a temperature range of -30~250 °C at a heating rate of 3 °C/min under nitrogen. DSC analysis was conducted at a heating rate of 10 °C/min on a Shimadzu DSC-50 thermal analyzer under nitrogen. Thermogravimetric analysis (TGA) was performed on a TA Instruments Hi-Res Modulated TGA 2950 analyzer under nitrogen or in air at a heating rate of 15 °C/min.

## RESULTS AND DISCUSSION

**Preparation of nano-composite emulsions**

Several series of NCEs consisting of acrylic resin and silica particles were prepared according to the previously reported method [27], which is briefly described in the

Experimental section. Here, three monomer compositions were chosen for the acrylic resins in preparing the NCEs; MMA: *n*-BA= 35:65, 50:50, and 65:35 (wt/wt%). The resultant emulsions consisted of hybrid particles of 50~60 nm in diameter, and in each of which a silica particle of 20~30 nm in diameter was surrounded by an acrylic layer cage. We also prepared silica-free acrylic emulsions having identical monomer compositions as control samples. Hereafter, these silica-free acrylic emulsions or the acrylic resins obtained from them are called ACn (x:y) where n denotes the sample number corresponding to the above monomer composition (x:y) of acrylic resin; MMA: *n*-BA= x: y as AC1 (35:65), AC2 (50:50), and AC3 (65:35). The NCEs are also named NCn-X by using the sample number (n) expressing its monomer composition of the acrylic resin (identical with the n of ACn) and its silica content (X) as NC2-1 (silica: acryl=35: 100 (w/w)), NC2-2 (silica: acryl=50: 100), and NC2-3 (silica: acryl=60:100). The same abbreviations are used for the films prepared from the emulsions, although we sometimes add a term, emulsion or film, after the abbreviation for easier understanding. The acrylic emulsion AC2 used for preparing NC2-X is currently utilized as the main component of the ordinary acrylic wall paints [28], whereas the acrylic compositions of AC1 and AC3 for preparing NC1-X and NC3-X are softer and harder, respectively, consisting of different n-BA compositions.

As reported before [27], the NCEs can be prepared by using a reactive nonionic surfactant NIS having a lower cloud point ($T_{cp}$) of 40 °C in the pre-polymerization step. This surfactant is first mixed with colloidal silica at temperature lower than the $T_{cp}$, and it is then allowed to deposit by raising the temperature to 60 °C that is significantly higher than the $T_{cp.}$ During this process, the depositing surfactant mostly sediments on the surface of the silica nano-particles to make an over-coat layer that can accommodate monomer layer in the initial pre-polymerization. Table 1 compares the typical preparations of acrylic emulsions in the presence and absence of NIS, which were selected from the data previously reported [27]. It

was evident that the acrylic emulsion finally obtained without adding a nonionic surfactant in the initial pre-polymerization (Run No.1) consisted of both large (158 nm in average diameter) and small particles (35 nm in average diameter) because of the presence of the un-coated silica particles (20-30 nm in average diameter). In this particular case, only an anionic surfactant SDS was used as the emulsifier which ought to have no specific interaction with silica particles. Use of the other anionic surfactants such as sodium alkyl diphenyl ether disulfonate (PELEX® SS-H, Kao Corp.), sodium polyoxyethylene alkyl ether sulfate (EMAL® D-3-D, Kao Corp.), and ammonium lauryl sulfate (LATEMUL® AD-25, Kao Corp.) gave similar results. Even by using a nonionic surfactant having higher $T_{cp}$ such as ADECA REASOAP® NE-30 ($T_{cp}$ > 100 °C, abbreviated as NIS-30), bi-modal size distribution of the emulsion particles was observed. The single modal size distribution of the emulsion particles was obtained only in the presence of NIS or other nonionic surfactants showing low $T_{cp}$ in which each silica nano-particle was enveloped to form a core-shell nano-particle. The use of the reactive surfactant NIS was effective for increasing the emulsion stability and not essential for constructing the acryl-silica core-shell structure in the NCE. The related unreactive nonionic surfactants showing low $T_{cp}$ were also effective for preparing the hybrid NCE.

Figure 1 compares the changes in solution states of an original colloidal silica solution (A: free of NIS), an aqueous solution of NIS (B), and a NIS-containing colloidal silica solution (C) with temperature variation. The colloidal silica (A) showed no change in appearance with the temperature change, keeping a colloidal state of white in color. In contrast, the solution of NIS (B) turned turbid on warming at 60 °C, and gel-like precipitates sedimented on the bottom part of the test tube when kept at 60 °C for 16 h because of the insoluble nature of the nonionic surfactant above $T_{cp}$. The precipitates, however, were quickly re-dissolved by cooling to room temperature. The colloidal silica containing NIS (C) became highly cloudy on warming at 60 °C and separated into two layers. The bottom layer consisted

of both NIS and colloidal silica particles, forming a soft gel. This phase-separated feature was not broken even when the system was cooled down to room temperature, i.e., below $T_{cp}$. These results indicated that the surfactant NIS depositing above $T_{cp}$ included the silica particles together and precipitated as gel. This gel state, once formed, did not turn to sol again even at higher temperature. The same behavior was also observed by using a non-reactive nonionic surfactants as EMULGEN® 108 (a polyoxyethylene lauryl ether obtained from Kao Corp. $T_{cp}$ = 40 °C), but not by using nonionic surfactants showing higher $T_{cp}$ such as EMULGEN® 120 ($T_{cp}$ = 98 °C) and 130K ($T_{cp}$ > 100 °C), both non-reactive polyoxyethylene lauryl ether-type made by Kao Corp. as well as by using reactive-type NIS-30 ($T_{cp}$ > 100 °C). With these nonionic surfactants, the surface deposition is not possible.

All the above results strongly suggest that the nonionic surfactants such as NIS can work as specific emulsifiers in the initial stage of polymerization to generate an organic thin layer on each of the colloidal silica particles that can efficiently allow the formation of NCE composite emulsions.

**Film-forming ability of the NCEs and film transparency**

Each of the NCEs obtained in the preceding section was fabricated into a film by the ordinary casting method using a polyethylene substrate. Table 2 summarizes the film-forming abilities of the NCEs. It is suggested here that the film formation depends on the balance of the softness related with the glass transition temperature ($T_g$) of the acrylic resins and the hardness related with the silica content.

The $T_g$ values of AC1 (MMA:*n*-BA=35:65), AC2 (50:50), and AC3 (65:35) were -4 °C, 21 °C, and 43 °C, respectively, as determined by the DSC analysis of the polymers. A general decreasing tendency of $T_g$ with increasing the n-BA content coincides with the order

of softness of the acrylic resins [29]. Since the AC1 was a gummy material, even NC1-1 and NC1-2 having low silica contents did not form self-supporting films. In these cases, the resulting films were too soft and sticky to be peeled off from the substrate. When the silica content was further increased, the films became enough rigid to be self-supporting. Thus, transparent films were successfully obtained from NC1-4 ~ NC1-7 in which the silica-to-acryl composition increased from 85 for NC1-4 to 150 (wt/wt%) for NC1-7. Above this composition, the film became too brittle to be crack-free, and NC-8, for example, having a silica-to-acryl composition of 175 (wt/wt%), could not be fabricated into a transparent film even on a polyethylene plate.

On the other hand, AC2 consisting of a harder polyacrylate (Tg = 21 °C) gave a transparent self-supporting film in silica-free state. The NCEs NC2-1, NC2-2, and NC2-3 could also be fabricated into similar transparent films whose silica-to-acryl compositions were in a range of 35-60 (wt/wt%), whereas no crack-free film was obtained from NC2 having a silica content higher than 60 (wt/wt%) because of the brittle nature. In the NC3 series consisting of a significantly hard polyacrylate, it was impossible to peel off a crack-free film at any of the silica-acryl compositions, although the as-formed films NC3-1~ NC3-3 having a silica-to-acryl composition up to 60 (wt/wt%) were all transparent (data are not involved). Even in the film of NC3-1 having the lowest silica-to-acryl composition of 35 (wt/wt%) crack formation attended when peeled off from the substrate. Since the hardest polymer AC3 (Tg = 43 °C) gave a brittle film, its involvement of silica nano-particles only enhanced the fragileness of the resulting film.

For comparison, simple silica-acryl blend emulsions were also prepared by mixing the AC emulsions and colloidal silica CS-50. Both the blend emulsions and their cast films are abbreviated as BLn-X where n and X denote the aforementioned sample number and silica content, respectively, as those of NCn-X. The film forming ability of BLn was not so

different from that of NCn at most of the acrylic compositions and silica contents. Significant difference was observed only for the blend films BL1-7 and BL2-3 having higher silica contents, which became more brittle than the corresponding NC films (NC1-7 and NC2-3) (Table 2).

Figure 2 compares the appearances of the NC1 and BL1 films having identical silica contents. The size of the glass substrate used for the film casting was 100×150 $mm^2$, and the average thickness of the film formed was 40~45 μm. While the BL1 film became translucent with white edges at a low silica-to-acryl composition of 125 (wt/wt%) and whole white above this composition, the NC1 film turned white in color at a silica-to-acryl composition as high as 200 (wt/wt%). Since the whitening is attributed to the aggregation of silica particles, the NC structure ought to be effective for suppressing the particle aggregation. It is because each silica particle is separated from each other with the core-shell structure. It is noteworthy that the volume content of silica is 47 % in the transparent NC1-8 film while it reaches 50 % in the white NC1-9 film. In the latter film, therefore, the amount of organic matrix may be below a critical level, making it difficult to keep the homogeneity of the hybrid particles. Consequently, the film forming ability of the NCE is strongly influenced by the silica content and the related soft/hard balance of the resultant composite films.

As reported elsewhere [27], the core-shell structure of NCE is effective for preventing the aggregation of silica particles and for homogeneous distribution of silica particles in making its cast film. In the present NCE, however, no covalent bonding is present between the silica surface and acrylic resin, and the silica particles are sometimes excluded out of the acrylic shells during the drying process of the cast films to form local aggregation structure. Probably, the cage of the silica particle is not strong because of the rubbery nature of acrylic resin consisting of higher n-BA compositions and the covering of the silica surface with the surfactant NIS. In fact, the FE-SEM photo of the surface of a NC1-4 film indicated several

particles agglomerated in several parts (shown by arrows in Figure 3 (a)). The TEM image also indicated such agglomeration, although the size of the agglomeration or the number of particles in direct aggregation is not so large (Figure 3 (b)) as that observed in the blend film prepared by mixing colloidal silica and acrylic emulsion. This difference in particle agglomeration causes the different properties of the cast films prepared from NC and BL emulsions.

**Tensile properties of NCE films**

We evaluated the mechanical properties of the films of NCn obtained above and compared with those of the corresponding BLn films. Figure 4 compares the representative stress-strain curves (S-S curves) of the NC1 and BL1 films. Since the basic polyacrylate AC1 of NC1 and BL1 was gummy at room temperature, its tensile properties could not be measured. Both NC1 and BL1 films involving silica nano particles became stronger with increasing the silica content. As indicated in Figure 4(a) (enlarged), the yield strength and strain of the BL1 films became higher and lower, respectively, with increasing the silica content (from BL1-4 to BL1-7). The NC1 films also exhibited similar behaviors, but their yield strength and yield strain were lower and higher, respectively, compared to those of the corresponding BL1 films having identical silica contents. NC1-4 showed much higher elongation than NC1-6 in spite of having a similar yield stress. Interestingly, each of the NC1 films showed a plateau region above the yield point, and the NC1-4 film containing 29 vol% of silica indicated a wide plateau region extending to over 400 % in strain, while the NC1-7 film containing 43 vol% of silica showed a very limited plateau region (c.a. 1 %). Since no plateau region was shown by the BL1 films, this elastic behavior shown above the yield point ought to be characteristic of the NC1 films in which the nano-particles are distributed more homogeneously with smaller particle agglomeration.

The tensile modulus, elongation, and strength of the NC1 and BL1 films are plotted as a function of silica content in Figure 5 (The numerical data are summarized in Table 3). Evidently, both the modulus and strength dramatically increased with increasing the silica content in both NC and BL films, while their elongation at break decreased oppositely. Little difference was observed in the tensile modulus and strength of the NC1 and BL1 films having identical silica contents. The increased mechanical properties can reasonably be attributed to the reinforcement effect of silica particles.

Figure 6 compares the representative S-S curves of the NC2 and BL2 films. Note that the base acrylic polymer AC2, having a $T_g$ at 21 °C (by DSC), showed a typical strain-stress behavior of the ordinary plastic films; the stress gradually increased from its yield point to its fracture point that reached 450 % in elongation. Both the NC2-3 and BL-2-3 films involving silica particles also showed similar behaviors, but their modulus became much higher and the elongation became lower.

As plotted in Figure 7 (The numerical data are summarized in Table 4), the tensile modulus increased with increasing the silica content while the elongation decreased oppositely, while the tensile strength was not much influenced by the silica content. Little difference was observed between the tensile properties of NC2 and BL2, probably because the hard or plastic nature of the matrix resin AC2 reflected them.

The above results revealed that only NC1-4 showed an interesting plastic region in the S-S curve. The drop of stress of the NC1 and BL1 films ought to be caused by the crazing taking place between the silica particles and the matrix polymer around the yield point. The silica particles in NC1-4 film, however, still retains strong interaction with the matrix even passing the yield point, probably because the nano-size silica particles may be involved in the entanglement of polymer chains and the silica-acrylic polymer chain interaction is to be maximum at this silica content as Espiard et al. suggested before [7]. In the corresponding

BL1 films, on the other hand, the dispersion state of the silica particles is not homogeneous, and the stress is likely to be concentrated on silica-poor parts after the yield point, causing the decreased stress with strain. In other words, the higher stress after the yield point of NC1 is another evidence for the well-dispersed state of silica particles in NC1.

**Dynamic mechanical properties of NC films**

Figure 8 shows typical DMA curves of the NC1 films. Evidently, the storage modulus (E') of the NC films became larger with increasing their silica content, particularly above $T_g$ of the acrylic resin which was determined to be 10 °C from the peak of tan δ curves (Figure 8b). Note that that the tan δ value decreased with increasing the silica content although no $T_g$ change was recorded with it. The reinforcement effect of silica is therefore clearly shown for the NC1 films.

Figure 9 shows the DMA curves of the NC2 and the related films. Different from the above AC1 polymer, the acrylic polymer AC2 exhibited a typical glassy feature in the DMA curve; E' dropped sharply around 50 °C correspondingly to the glass-rubber transition. From the tan δ peak, the $T_g$ of AC2 was determined to be 54 °C (Figure 9b). The E' of NC2 containing silica particles was higher than that of AC2, especially, above the $T_g$. For example, the E' values of NC2-1 and NC2-3 were about 3.7 MPa and 19 MPa, respectively, at 80 °C, while that of AC2 was about 1.0 MPa. Below $T_g$, however, the increase in modulus of NC2 was rather limited (from 1.6 GPa of AC2 to 2.8 GPa of NC2-3 at -20 °C). No clear Tg change was also shown here. Similar hybridization effects on the Tg and E' changes were ever reported for butyl acrylate/styrene copolymer containing nano silica particles [30]. For the simple blend films BL2, the effect of nano silica on the E' change was much smaller, and the E' change exhibited irregular peaks (see Figure 9 for BL2-3), which may be attributed to the inhomogeneous distribution or the large local aggregation of the particles in the blend films.

**Thermal resistivity of the NCE films**

Typical TGA curves of the NC1, NC2, and the related films are compared in Figure 10. The thermal data involving the temperatures of 5 ($T_{5\%}$) and 10 wt% losses ($T_{10\%}$) are determined from these curves and summarized in Table 5. Both AC1 and AC2 started to decompose around 300 °C and almost lost their weight at 410 °C in nitrogen atmosphere. They showed similar $T_{5\%}$ and $T_{10\%}$ values both in nitrogen and in air, although the values were slightly lower in air. On the other hand, the $T_{5\%}$ and $T_{10\%}$ of NC1-3 in nitrogen were 308 and 335°C, respectively, whereas those of NC2-2 were 349 and 364°C, respectively. NC1-3 showed a considerably faster initial weight loss. In air, the same values ($T_{5\%}$ and $T_{10\%}$) of NC1-3 and NC2-2 were (277 and 294°C) and (275 and 285°C) as shown in combination, respectively, being even lower than those of AC1 and AC2 in air, although the residual weights of NC1-3 and NC2-2 at 500 °C were as high as 36-37 wt% and 32-33 wt%, respectively. These residual weights were almost coincident with their silica contents, 38 and 33 wt%, respectively, indicating that silica components had remained without decomposition up to 500 °C. Since the silica particles (involved in Figure 10a) showed a small weight loss (4.7 wt% at 100°C and 6.0 wt% at 500 °C) due to the silanol condensation at surface, their weight loss may have contributed to the relatively fast weight losses of NC1-3 and NC-2-2. Assuming that the silica particles have no special effect on the thermal degradation of the acrylic polymer, an ideal TGA curve of NC1-3 could be predicted by combining the TGA curves of AC1 and silica particles with their weight fraction considered. Figure 11 compares the real TGA curves of NC1-3 with the predicted curves. Evidently, the weight loss of NC1-3 was lower than the predicted below 300 °C. This difference may be attributed to the degree of homogeneity in dispersion state of the particles by which the silanol condensation among the silica nano-particles can be reduced. In the NC1, the silica

surface must effectively be covered with nonionic surfactant, suppressing the rate of silanol condensation [28]. Above 300 °C, in return, NC1-3 showed larger weight loss than predicted, especially under nitrogen. Probably, the acidic silanol groups on the silica particles may have accelerated the decomposition of acrylic matrix. It was also shown here that the decomposition proceeds much faster in air than in nitrogen.

The initial weight losses of AC2 at 100 and 200 °C in nitrogen reached 0.7 and 0.9 %, respectively, which were significantly higher than the corresponding values of AC1 (Figure 10b). It is considered that the higher $T_g$ of AC2 may have hindered the migration of water through the film during the drying process to increase the water content in the resulting film.

As shown in Figure 11, the weight loss of NC1-3 below 250 °C was lower than the predicted one. The residual weights of NC1-3 at 500 °C were 37 % in nitrogen and 36 % in air, which were almost coincident with its silica content, 38 %, again. As noted in Table 5, the blend film BL2-2 exhibited higher weight losses than NC2-2 below 200 °C, suggesting the silanol condensation induced among the silica particles in agglomeration in the film. Consequently, the homogeneity of the NCE films in terms of particle distribution is very efficient for the decreased weight loss below 250 °C or for increasing the thermal stability.

As described previously [29], a white paint prepared by using NC1-type hybrid emulsion showed characteristic anti-flaming property. This property must be attained not only by its low organic content but also by the moisture formation from silica particles of upon heating, whose rate should efficiently be slowed down in the NCE structure.

## CONCLUSION

Various NCE films were prepared from hybrid emulsions incorporating a nano-size silica particle in the emulsion core. Among them, NC1-3~6 containing 60-150 wt/wt %

silica relative to acrylic resin were found to have both stiffness and toughness enough to be utilized for practical purposes such as paint resins. DMA analysis supported their relatively high tensile modulus at high temperature. TGA analysis also assured their heat-resistance up to 250 °C, although the incorporated silica slightly accelerated thermal decomposition of the acrylic resin above 250 °C in air. It was confirmed that the NC films are generally superior to the BL films directly prepared by mixing colloidal silica and acrylic emulsion in terms of the homogeneity of particle distribution in the cast films as well as of the mechanical strength at high temperature. The transparency of the NC films was excellent, being very important for application of these materials to proper color decoration. It was also revealed that the nonionic surfactant NIS is allowed to sediment on the colloidal silica surface above its clouding point, forming an organic thin layer that can work as the site for monomer adsorption and polymerization.

Contrary to the conventional acrylic emulsion whose solid part is almost exclusively derived from the petroleum resources, the solid part of the present NCE contains up to 60 wt% of silica. The usage of such a new composite material as architectural paint is effective for reducing the consumption of the petroleum resources in the field of paint industry. The reduction of organic content in paints is also efficient for reducing the emission of $CO_2$ by their incineration after use, considering that paints, once processed, cannot be recycled.

**Table 1. Typical emulsion polymerizations of an acrylics/silica mixture with different surfactants [a)]**

| Run No. | Nonionic surfactant (Tc) | Yield (%) | Appearance [b)] | | Av. Diameter [c)] (nm) |
|---|---|---|---|---|---|
| | | | Just after preparation | After 1 day | |
| 1 | None [d)] | 98 | h.e. | h.e. | 35±6, 158±46 |
| 2 | NE-10 (40 °C) | 100 | h.e. | h.e. | 111±54 |
| 3 | NE-30 (>100 °C) | 100 | p.a.e. | gel | 98±15, 630±200 |

[a)] Polymerization conditions: identical with that described in the Experimental section. Feed ratio: silica/acrylic monomers 85/100 (wt/wt) with AT 50 (340 g), MMA (130 g), BA (69 g), MAA (1 g), nonionic (NE-10 or 30) (4 g), SDS (24 g), and water (140 g)) Initiator: APS. Temperature: 60-70 °C.

[b)] h.e., homogeneous emulsion; p.a.e., partly aggregated emulsion.

[c)] Determined by DLS in which the Marquadt method was used for analysis.

[d)] By the use of anionic surfactants only.

**Table 2. Film forming abilities of the nano-composite emulsions.** [a)]

| Silica content | | | MMA: *n*-BA=35 :65 (w/w) | | | | MMA: *n*-BA=50: 50 (w/w) | | | |
|---|---|---|---|---|---|---|---|---|---|---|
| | | | NC film | | BL film | | NC film | | BL film | |
| Silica : Acryl (wt: wt) | | (vol-%) | Sample | Film forming ability[b)] | Sample | Film forming ability[b)] | Sample | Film forming ability[b)] | Sample | Film forming ability[b)] |
| 0 : | 100 | 0 | AC1 | –(s) | | | AC2 | + | | |
| 35 : | 100 | 15 | NC1-1 | –(s) | BL1-1 | –(s) | NC2-1 | + | BL2-1 | + |
| 50 : | 100 | 20 | NC1-2 | –(s) | BL1-2 | –(s) | NC2-2 | + | BL2-2 | + |
| 60 : | 100 | 23 | NC1-3 | + | BL1-3 | + | NC2-3 | + | BL2-3 | ± |
| 85 : | 100 | 29 | NC1-4 | + | BL1-4 | + | NC2-4 | –(b) | BL2-4 | –(b) |
| 100 : | 100 | 33 | NC1-5 | + | BL1-5 | + | NC2-5 | –(b) | BL2-5 | –(b) |
| 125 : | 100 | 38 | NC1-6 | + | BL1-6 | + | NC2-6 | –(b) | BL2-6 | –(b) |
| 150 : | 100 | 43 | NC1-7 | + | BL1-7 | ± | NC2-7 | –(b) | BL2-7 | –(b) |
| 175 : | 100 | 47 | NC1-8 | –(b) | BL1-8 | –(b) | | | | |
| 200 : | 100 | 50 | NC1-9 | –(b) | BL1-9 | –(b) | | | | |

a) **A sample emulsion was cast on a PE plate and dried at 50 ℃ for 16h.**

b) **+: The film was successfully prepared.**

**±: The film was somewhat brittle, but it could be peeled off from the PE plate to obtain a crack-free film.**

**–(s): The substance was soft and sticky.**

**–(b): The film was too brittle to peel off from the PE plate.**

**Table 3. Mechanical properties of NC1 and BL1 films[a)]**

| Sample | Silica content Silica : Acryl (wt:wt) | Silica content (vol-%) | Tensile modulus (MPa) | Yield strain (%) | Yield stress (MPa) | Tensile elongation (%) | Tensile strength (MPa) |
|---|---|---|---|---|---|---|---|
| NC1-3 | 60 : 100 | 23 | 25±8.1 | 7.5 | 0.77 | 720±59 | 0.78±0.040 |
| NC1-4 | 85 : 100 | 29 | 230±25 | 3.3 | 1.7 | 770±64 | 3.6±0.066 |
| NC1-5 | 100 : 100 | 33 | 360±8.4 | 2.5 | 3.2 | 390±48 | 3.2±0.18 |
| NC1-6 | 125 : 100 | 38 | 220±38 | 2.2 | 3.4 | 10±2.0 | 3.4±0.11 |
| NC1-7 | 150 : 100 | 43 | 350±19 | 2.0 | 5.8 | 2.8±0.65 | 5.8±0.15 |
| BL1-3 | 60 : 100 | 23 | 25±7.9 | 10 | 0.78 | 510±50 | 0.78±0.060 |
| BL1-4 | 85 : 100 | 29 | 187±6.8 | 4.2 | 1.6 | 1200±120 | 3.8±0.29 |
| BL1-5 | 100 : 100 | 33 | 220±60 | 2.3 | 3.4 | 170±61 | 3.3±0.29 |
| BL1-6 | 125 : 100 | 38 | 270±50 | 2.2 | 5.2 | 2.5±0.44 | 5.2±0.19 |
| BL1-7 | 150 : 100 | 43 | 380±27 | 1.3 | 6.9 | 1.5±0.14 | 6.9±0.76 |

a) At a drawing rate of 30 mm/min.

## Table 4. Mechanical properties of NC2 and BL2 films [a)]

| Sample | Silica content | | Tensile modulus | Tensile elongation | Tensile strength |
|---|---|---|---|---|---|
| | Silica : Acryl (wt : wt) | (vol-%) | (MPa) | (%) | (MPa) |
| AC2 | 0 : 100 | 0 | 50 | 300 | 8.4 |
| NC2-1 | 35 : 100 | 15 | 102 | 240 | 6.4 |
| NC2-2 | 50 : 100 | 20 | 51 | 330 | 8.3 |
| NC2-3 | 60 : 100 | 23 | 280 | 200 | 8.3 |
| BL2-1 | 35 : 100 | 15 | 187 | 200 | 5.8 |
| BL2-2 | 50 : 100 | 20 | 75 | 290 | 7.3 |
| BL2-3 | 60 : 100 | 23 | 260 | 340 | 9.9 |

a) Elongation rate; 30min/min.

**Table 5. TGA data of nano-composite films.**

| | | In $N_2$ | | | | | In air | | | | |
|---|---|---|---|---|---|---|---|---|---|---|---|
| Sample | Silica content (wt%) | Weight loss (wt%) at 100°C | Weight loss (wt%) at 200°C | $T_{5\%}$[a] (°C) | $T_{10\%}$[b] (°C) | residual weight at 500°C (%) | weight loss (wt%) at 100°C | weight loss (wt%) at 200°C | $T_{5\%}$[a] (°C) | $T_{10\%}$[b] (°C) | residual weight at 500°C(%) |
| silica | 100 | --- | --- | --- | --- | --- | 4.0 | 5.0 | 192 | >500 | 94 |
| AC1 | 0 | 0.2 | 0.3 | 347 | 363 | 2.5 | 0.3 | 0.6 | 297 | 310 | 1.5 |
| NC1-3 | 38 | 0.9 | 1.3 | 308 | 335 | 37 | 0.9 | 1.4 | 277 | 294 | 36 |
| AC2 | 0 | 0.7 | 0.9 | 350 | 368 | 2.7 | 0.6 | 2.1 | 297 | 307 | 0 |
| NC2-2 | 33 | 0.7 | 1.1 | 349 | 364 | 33 | 0.8 | 2.5 | 275 | 285 | 32 |
| BL2-2 | 33 | 1.1 | 1.5 | 348 | 365 | 34 | 2.9 | 4.2 | 266 | 283 | 32 |

[a] Temperature at 5% weight loss.

[b] Temperature at 10% weight loss.

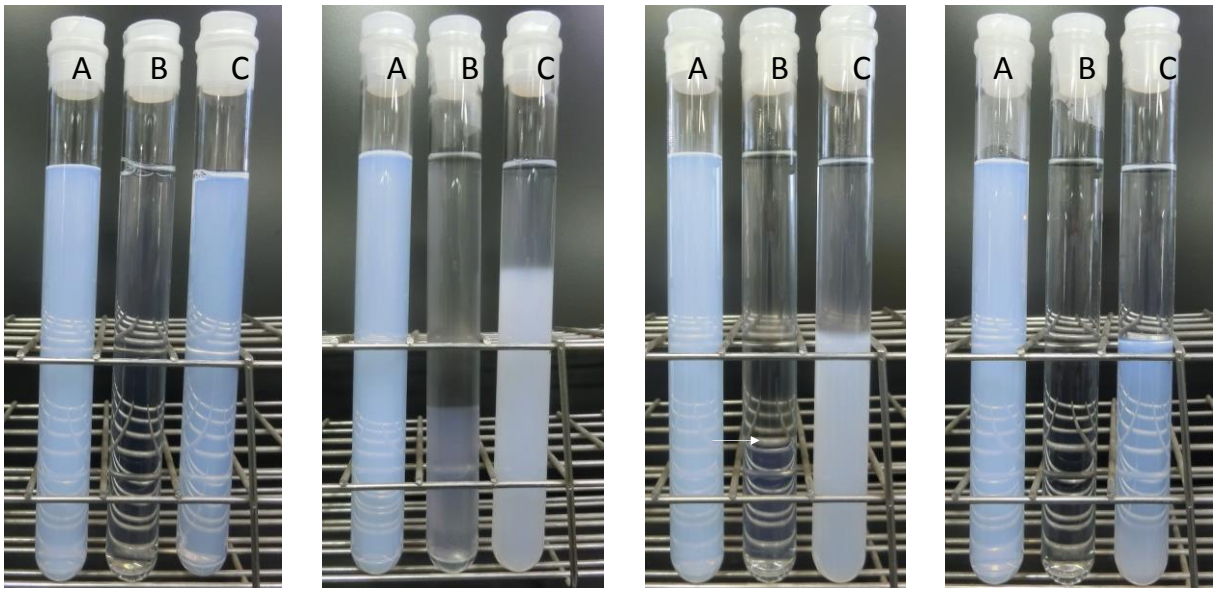


(1) Initial stage (r.t.) (2) At 60 ºC for 1 h (3) At 60 ºC for 16 h (4) Cooled to r.t.

**Figure 1. Temperature-dependent solution states of a colloidal silica (A: 33.4 wt-% in solid content), an aqueous solution of NIS (B: 5 wt-%-concentration), and a mixed solution (C) of colloidal silica (33.4 wt-%) and NIS (12 wt-%). The arrow shows the interface below which sediments are present.**

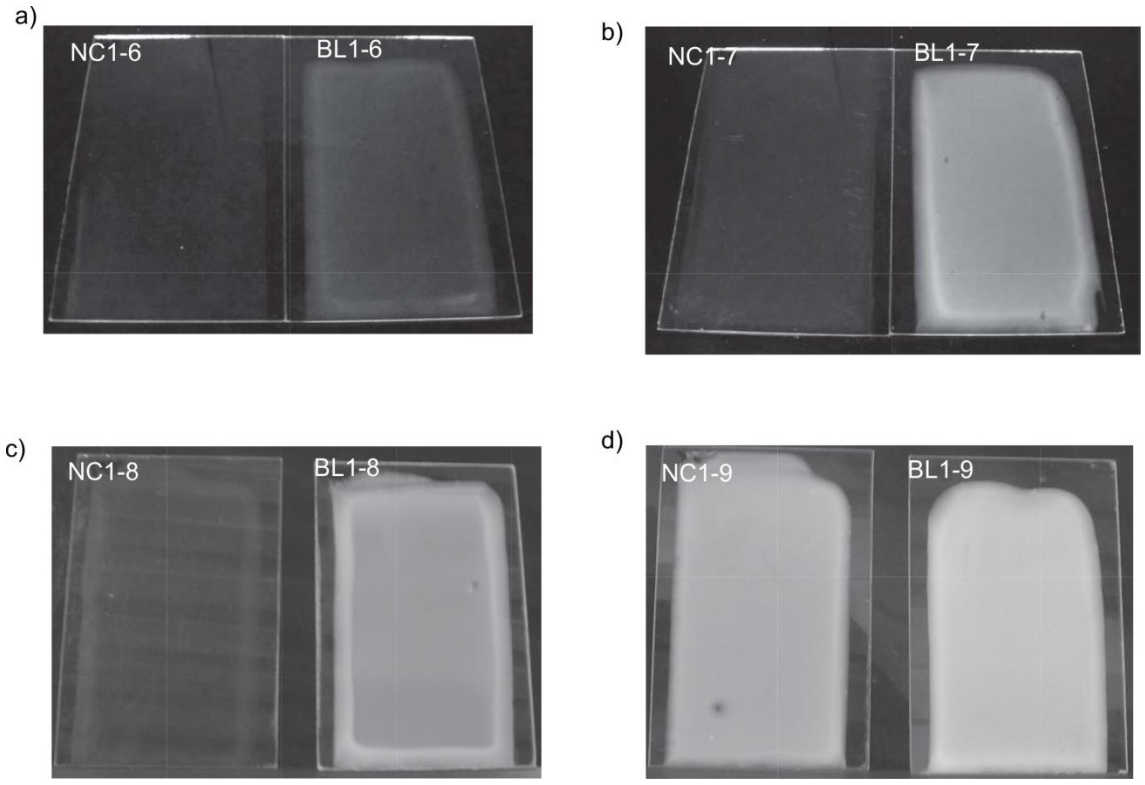


**Figure 2. Comparison of the appearances of NC1 and BL1 films.**

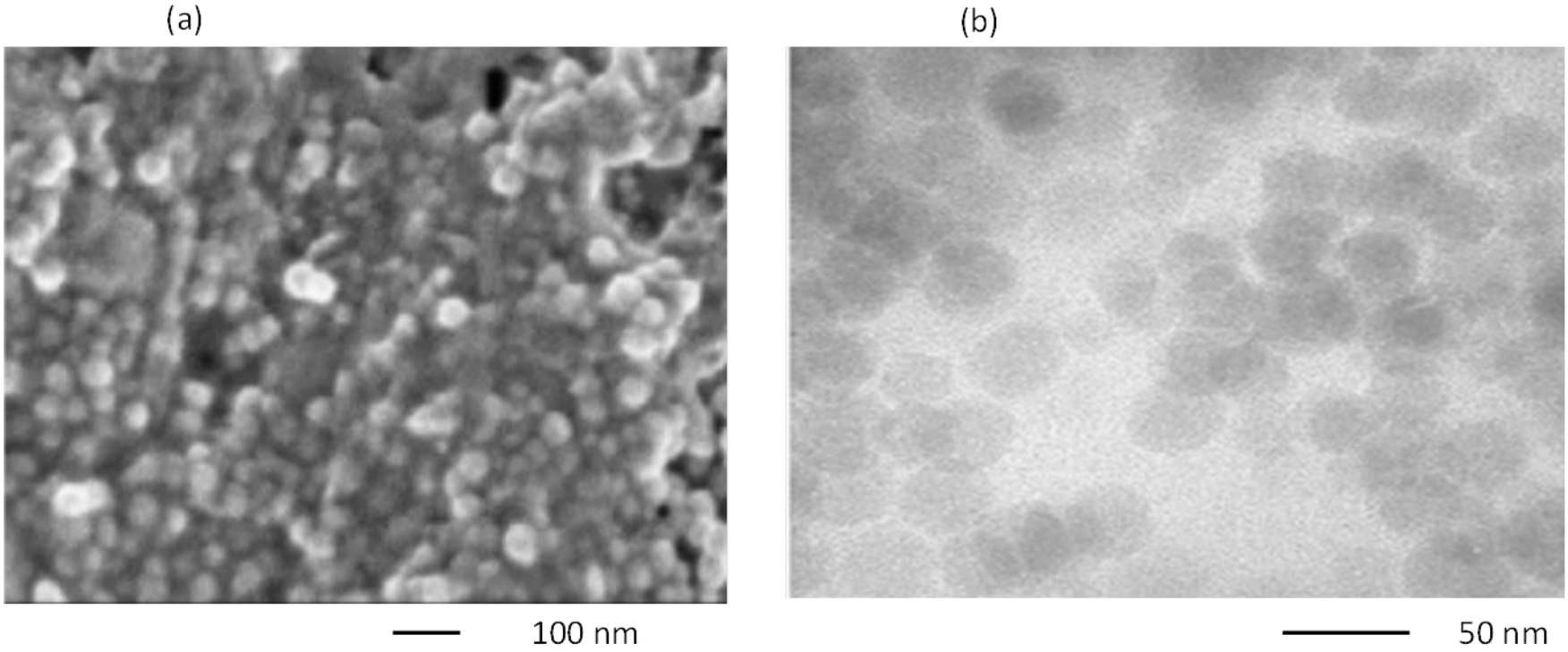


**Figure 3. Typical (a) FE-SEM (x 50,000) and (b) TEM (x 200,000) images of a cast film of NC1-4.**

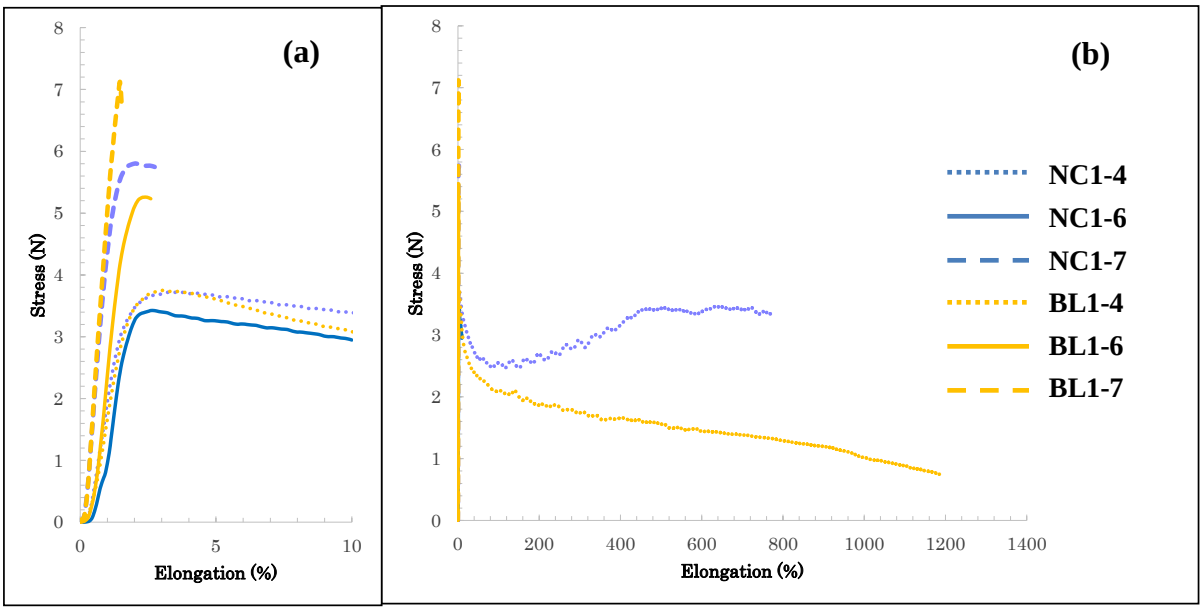


**Figure 4. Stress-strain curves of NC1 and BL1 films. The left (a) is the enlarged view of the right (b).**

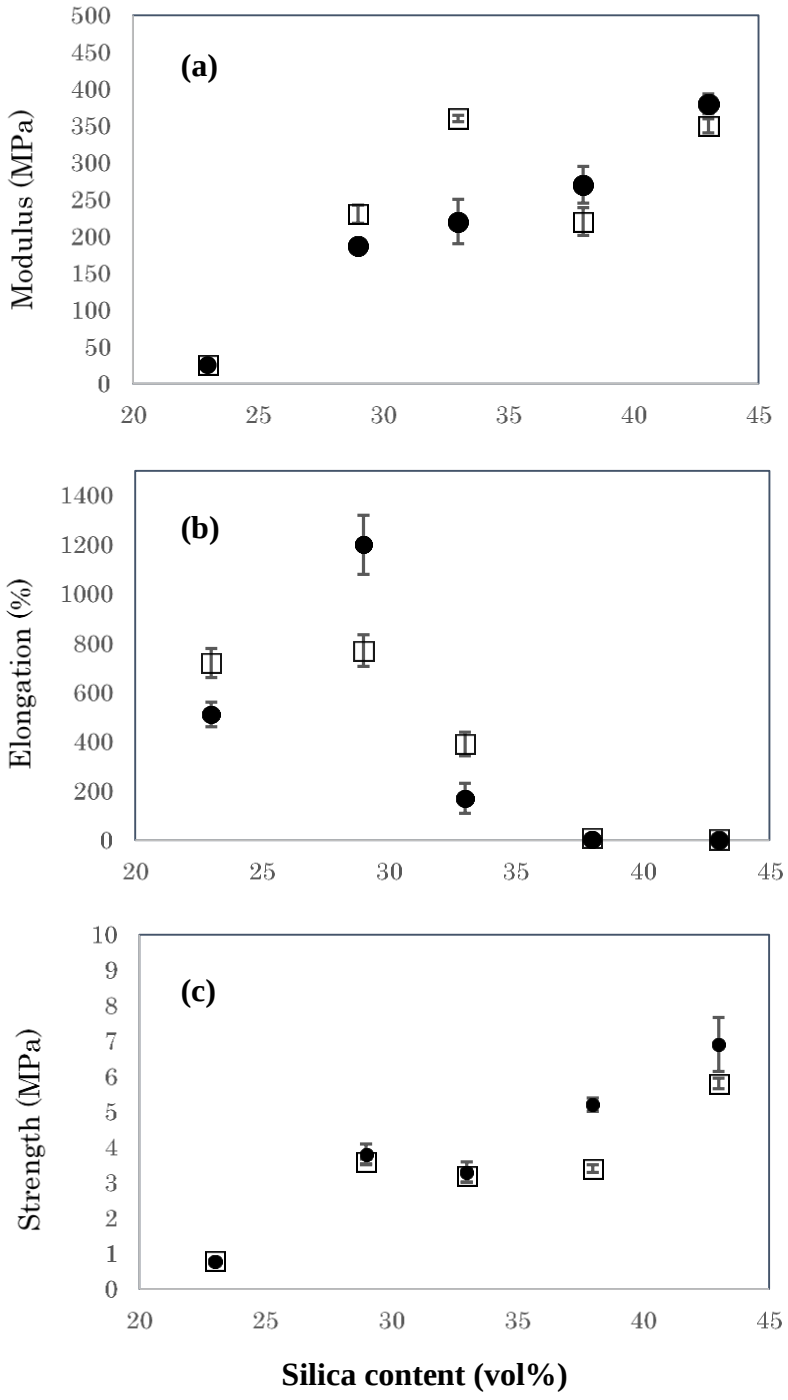


**Figure 5. Changes in (a) tensile modulus, (b) elongation, and (c) strength as a function of silica particle content for NC1 (□) and BL1 (●) films. The error bars are for average differences from the averaged values.**

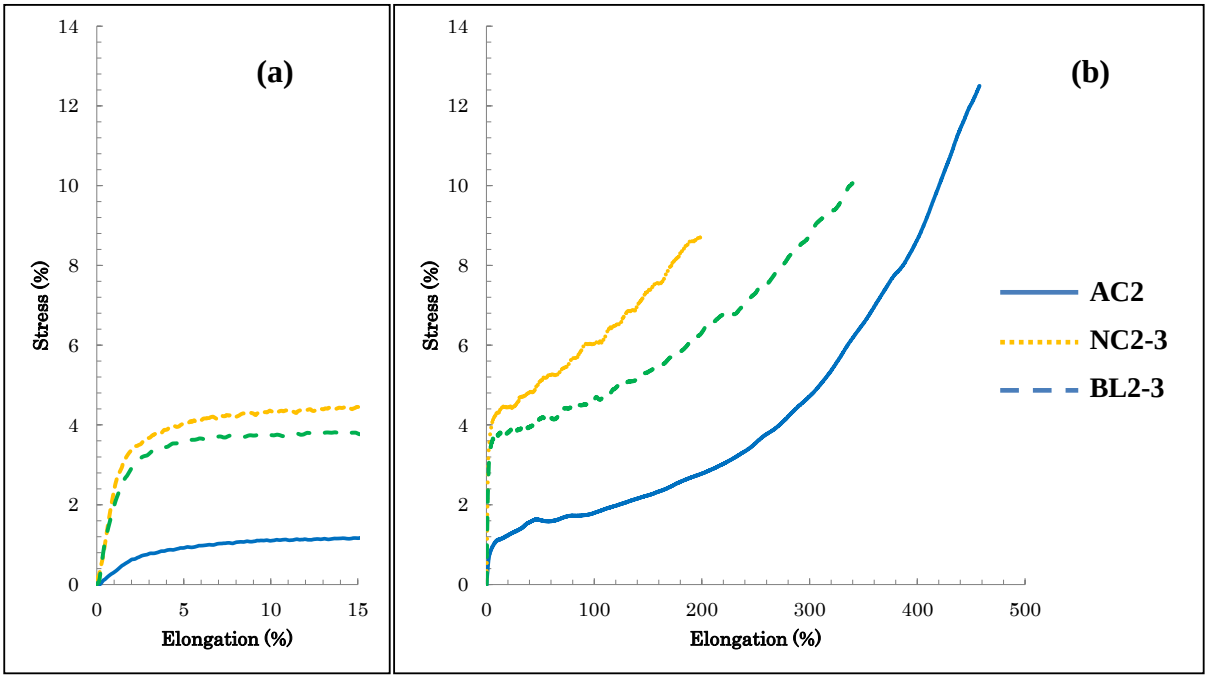


**Figure 6. Stress-strain curves of the NC2, BL2, and AC2 films. The left (a) is the enlarged view of the right (b).**

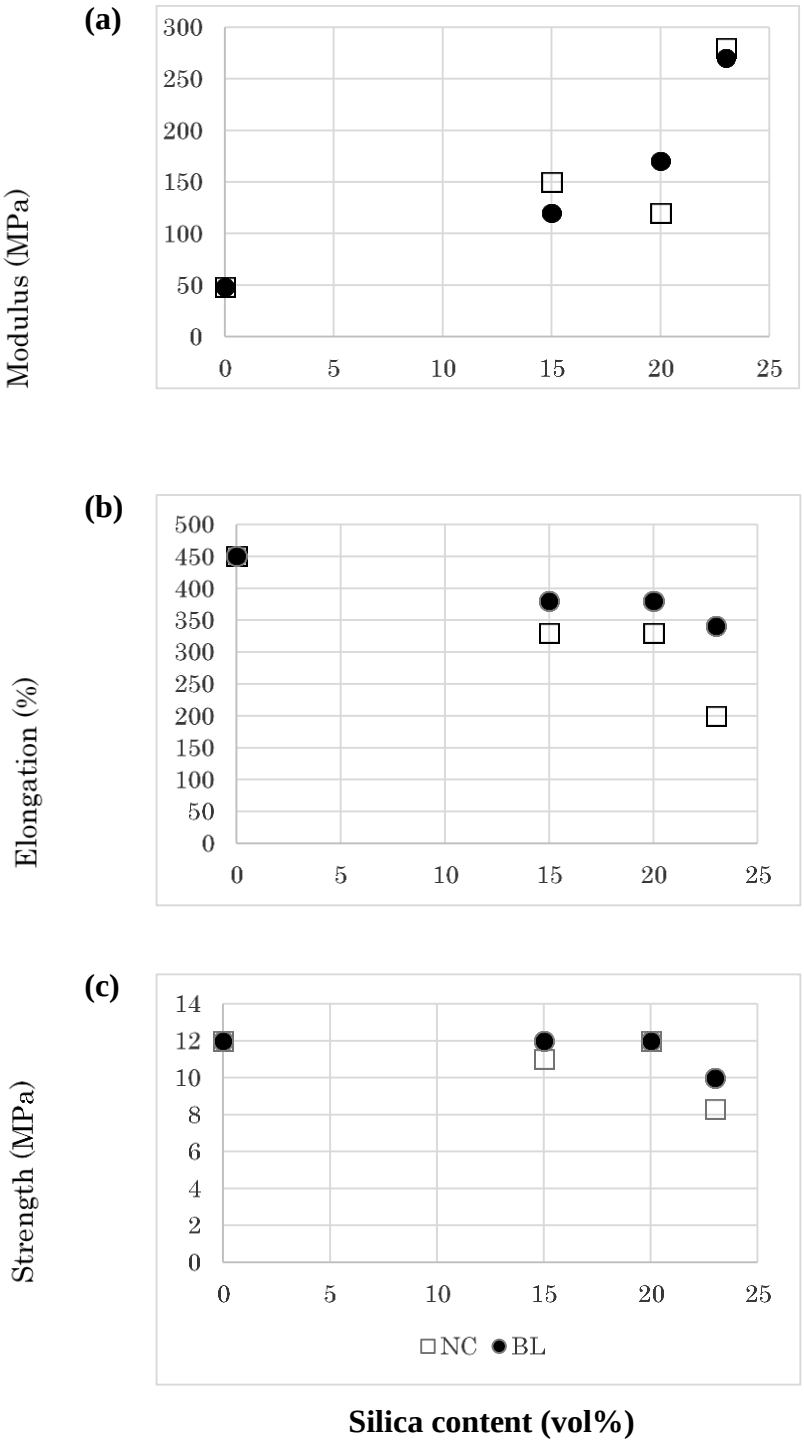


**Figure 7. Changes in (a) tensile modulus, (b) elongation, and (c) strength as a function of silica particle content for NC2 (□) and BL2 (●) films.**

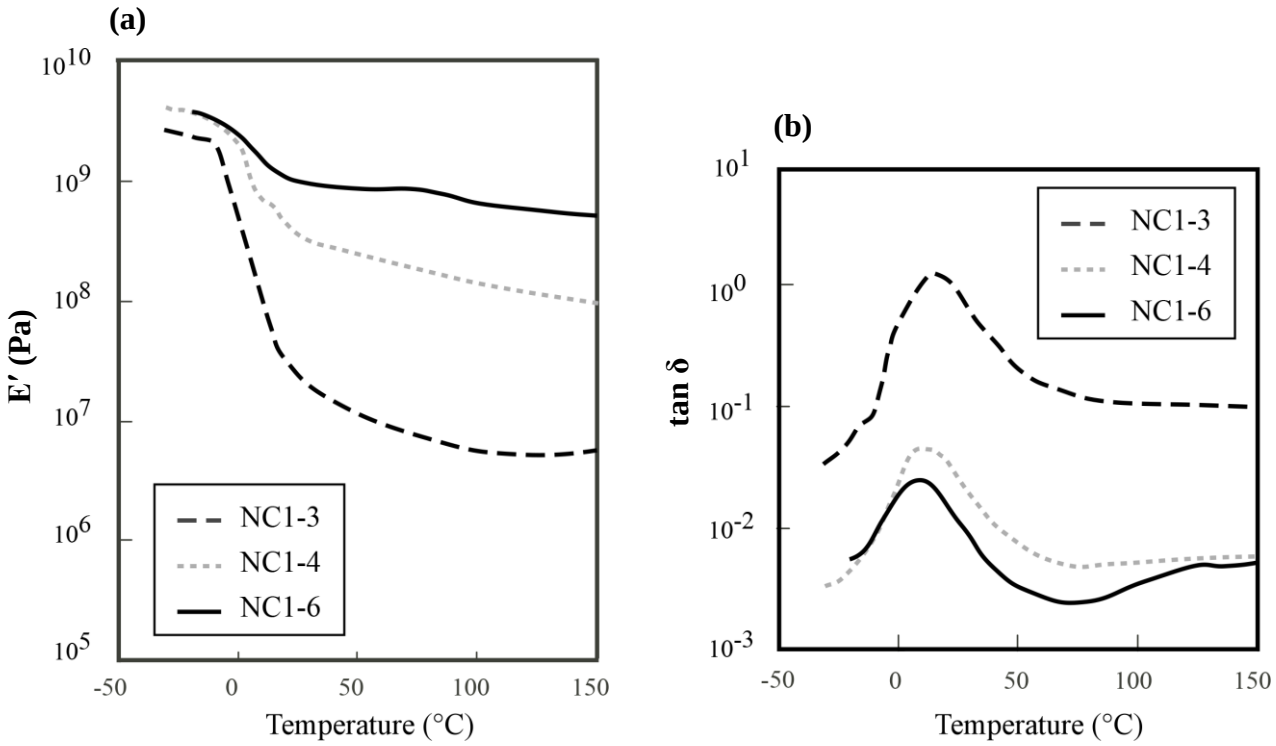


**Figure 8. Temperature dependences of storage modulus (a) and loss tangent (b) of the NC1 films.**

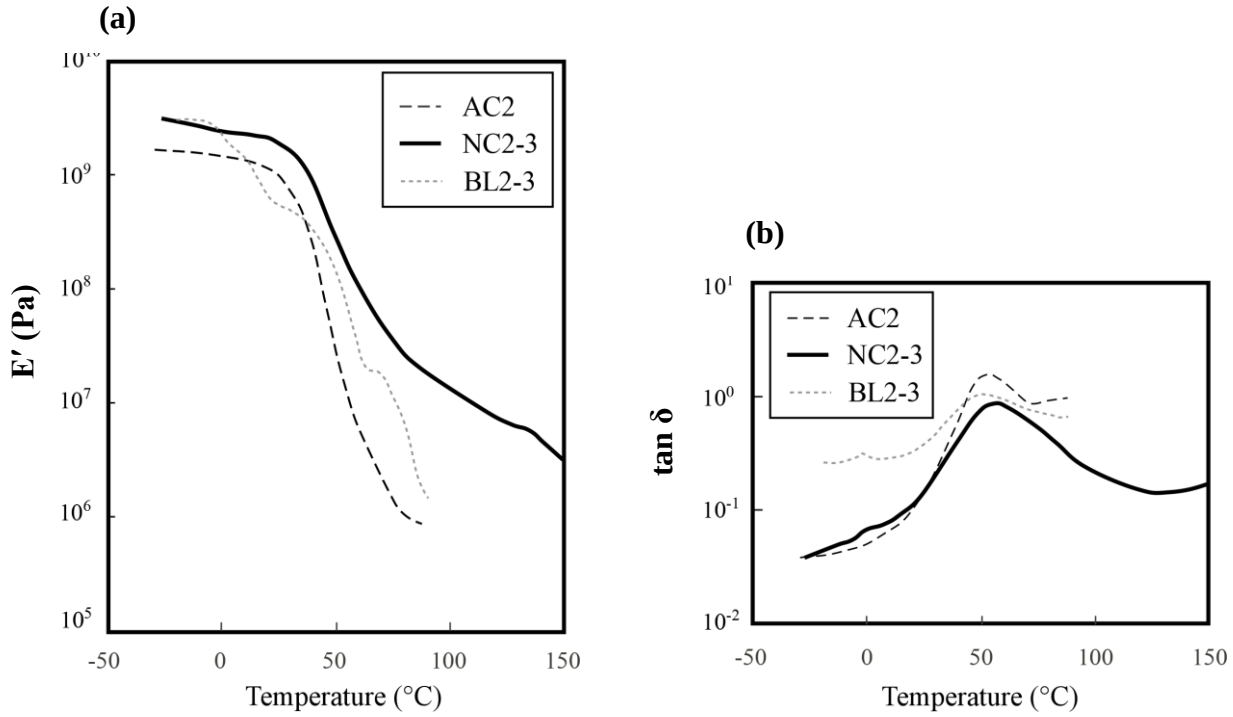


**Figure 9. Temperature dependences of storage modulus (a) and loss tangent (b) of the AC2-based films.**

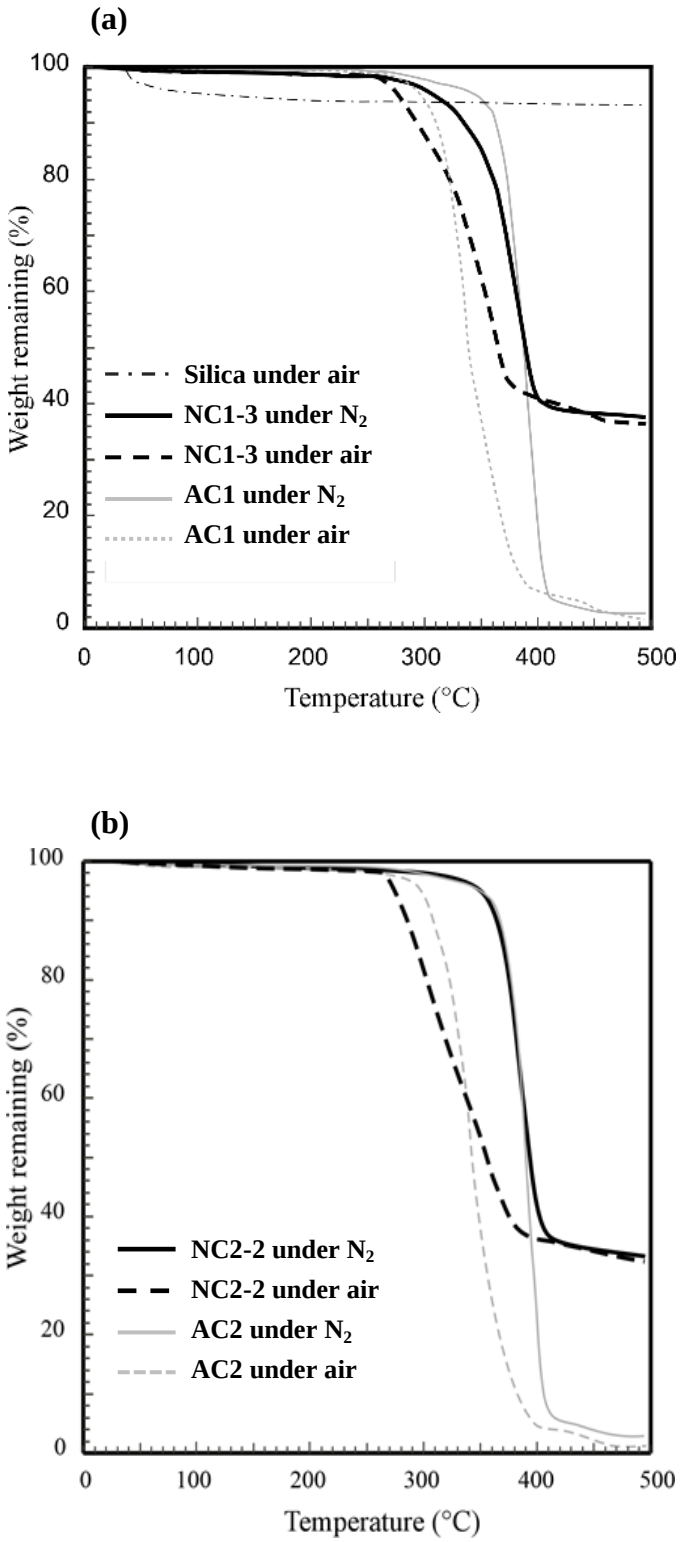


**Figure 10. TGA thermograms of (a) NC1-3 and (b) NC2-2 as compared with those of their related polymers and silica.**

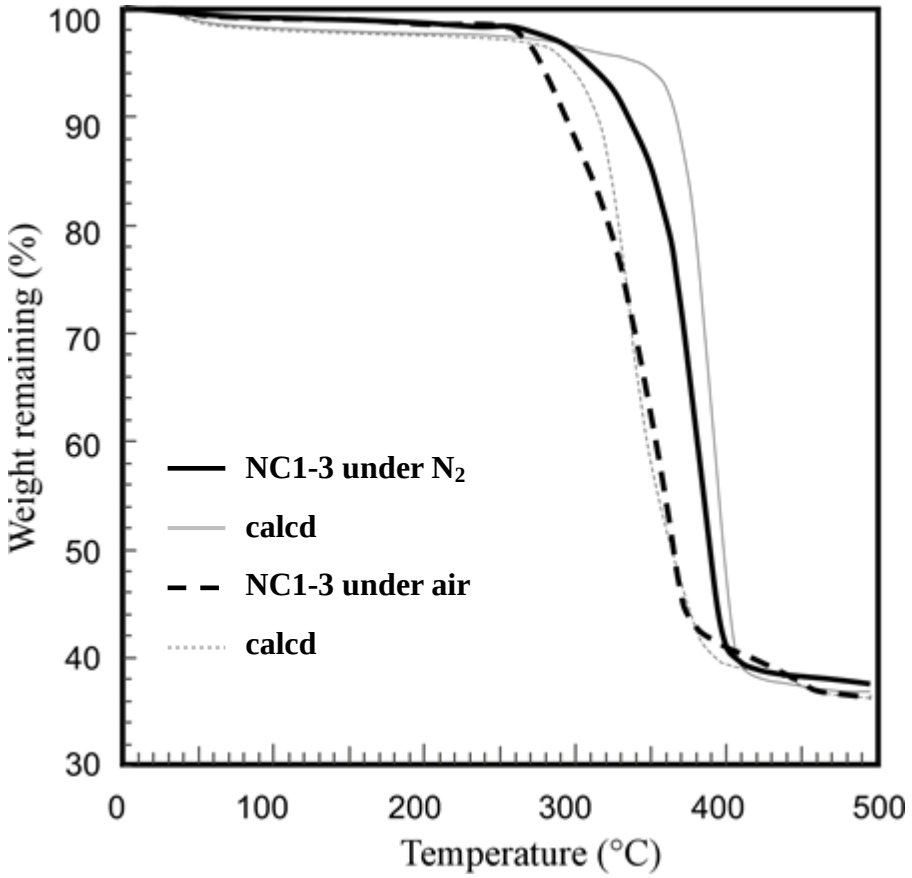


**Figure 11. Comparison of the real TGA thermograms of NC1-3 and the theoretically predicted ones from those of AC1 and silica particles in nitrogen and in air.**

## REFERENCES


1. J. L. Luna-Xavier, E. Bourgeat-Lami, A. Guyot, *Colloid Polym. Sci*., **279**. 947 (2001).
2. J. Lee, M. Sena, *Colloid Polym. Sci*., **273**,76 (1995).
3. K. Furusawa, K. Nagashima, C. Anzai, *Colloid Polym. Sci*., **272**,1104 (1994).
4. M. S. Fleming, T. K.Mandal, D. R.Walt, *Chem. Mater*., **13**, 2210 (2001).
5. For a review, see F. Caruso, *Adv. Mater*., **13**, 11 (2001).
6. Ph. Espiard, A. Guyot, *Polymer*, **36**, 4391 (1995).
7. Ph. Espiard, A. Guyot, J. Perez, G. Vigier, L. David, *Polymer*, **36**, 4397 (1995).
8. F. Tiarks, K. Landfester, M. Antonietti, *Langmuir*, **17**, 5775 (2001).
9. B. Erdem, E. D. Sudol, V. L. Dimonie, M. El-Aasser, *J. Polym. Sci. Polym. Chem.*, **38**, 4419 (2000).
10. R. Hashemi-Nasab, S. M. Mirabedini, *Prog. Org. Coat.*, **76**, 1016(2013)
11. E. Duguet, M. Abboud, F. Moravan, P. Maheu, M. Fontanille, *Macromol. Symp*., **151**,365 (2000).
12. J. Stejskal, P. Kratochvil, S. P. Armes, S. f. Lascelles, A. Riede, M. Helmstedt, J. Prokes, I. Krivka, *Macromolecules,* **29**, 6814 (1996).
13. K. Sooklal, L. H. Hanus, H. J. Ploehn, C. J. Murphy, *Adv. Mater*., 10, 1083 (1998).
14. L. Qi, H. Co¨lfen, M. Antonietti, *Nano Lett.*, 1, 65 (2001).
15. H. Zhao, E. P. Douglas, B. S. Harrison, K. S. Schanze, *Langmuir*, **17**, 8423 (2001).
16. R. C. Hedden, B. J. Bauer, A. P. Smith, F. Gröhn, E. Amis, *Polymer*, **43**, 5473 (2002).
17. B. You, N. Wen, Y. Cao, S. Zhou, L. Wu, *Polym. Int.*, **58**, 519(2009)
18. Z. Buhin, S. L. Blagojevic, M. Leskovac, *Polym. Eng. Sci.*, **53**, 2292(2013)
19. A. Dashtizadeh, M. Abdouss, H. Mahdavi, M. Khorassani, *Appl. Surf. Sci.*, **257**, 2118(2011)

20. M. Z. Rong, M. Q. Zhang, Y.X. Zheng, H.M. Zeng, K. Friedrich, *Polymer*, **42**, 3301 (2001).

21. J. Yuan, S.Zhou, G. Gu, L. Wu, *J. Mater. Sci.*, **40**, 3927 (2005).

22. K. G. Gatos, L. Szazdi, B. Pukanszky, J. Karger-Kocsis, *Macromol. Rapid Commun.*, **26**, 915 (2005).

23. S. Poompradub, S. Kohjiya, Y. Ikeda, *Chem. Lett.*, **3**4, 672 (2005).

24. F. Bauer, H.-J. Glaesel, E. Hartmann, H. Langguth, R. Hinterwaldner, *Int. J. Adhes. Adhes*., **24**, 519 (2004).

25. X. Huang, J. Zhong, C. Gong, *Mater. Lett.*, **58**, 1189 (2004).

26. R. Sengupta, A. Bandyopadhyay, S. Sabharwal, T. K. Chaki, A. K. Bhowmick, *Polymer*, **46**, 3343 (2005).

27. T. Mizutani, K. Arai, M. Miyamoto, Y. Kimura, *J. Appl. Polym. Sci.*, **99**, 659 (2006).

28. S. T. Eckersley, A. Rudin, *J. Coatings Technol.*, **62**, 89 (1990).

29. T. Mizutani, K. Arai, M. Miyamoto, Y. Kimura, *Prog. Org. Coat.*, **55**, 276 (2006).

30. M. Xiong, L. Wu, S. Zhou, B. You, *Polym. Int.,* **51**, 693 (2002).

# Chapter 2

## Colloidal silica bearing thin polyacrylate coat: A facile inorganic modifier of acrylic emulsions for fabricating hybrid films with least aggregation of silica nanoparticles

## INTRODUCTION

Much attention has been paid to hybrid nanoparticles in which inorganic nanometer-size particles are encapsulated by organic polymers in a form of core/shell structure. [1] These organic–inorganic hybrid nanoparticles are efficiently utilized as building blocks in preparing hybrid films with intriguing physicochemical properties that are originated from specific interfacial interactions between the inorganic nanoparticles and matrix polymer. [2,3] One of the most convenient methods for incorporating nanoparticles into a polymer matrix of nanoscale is to use miniemulsion polymerization in which monomer droplets of c.a., 50 to 500 nm in diameter suitably incorporate nanoparticles to achieve the encapsulation by polymerization. Landfester [4], Wu et al. [5], and Cao et al. [6] separately reviewed various miniemulsion processes for synthesizing such hybrid nanoparticles. In these processes, surface modification of nanoparticles is essential to increase the compatibility of inorganic nanoparticle surface with organic monomer for the successful encapsulation [7]. However, as Bourgeat-Lami et al. reported [8], the inorganic particle distribution in the resultant miniemulsion is not homogeneous even when the surface-modified nanoparticles are dispersed in acrylic monomer phase. Namely, the resultant emulsion likely involves free organic particles missing the inorganic cores together with hybrid particles including several inorganic cores [9]. Furthermore, highly effective sonication or high-pressure homogenization is required for emulsification of mini-droplets loaded with nanoparticles [10]. Therefore, this method may not readily be utilized in large-scale industrial production of hybrid particles.

The present author et al. previously succeeded in obtaining colloidal silica/polyacrylate hybrid particles by the ordinary emulsion polymerization method with the aid of a nonionic surfactant showing a lower critical solution temperature (LCST) or

cloud point ($T_{cp}$). In this method, each of the colloidal silica particles of 20~50 nm in diameter was covered with a polyacrylate coat of ca. 15~20 nm in thickness in a core/shell form. The resultant emulsion was accordingly called "nano-composite emulsion (NCE)" [11, 12]. Later, another group also traced the same method to obtain NCE [13]. In our real procedure (steps (A) and (B) in Scheme 1), an aqueous dispersion of silica nano-particles (colloidal silica) was mixed with such a nonionic surfactant and warmed up above its $T_{cp}$ with stirring to make the surfactant deposit on the surface of the colloidal silica particles. Then, a small amount of monomer was adsorbed on the surface of the surfactant-deposited particles and polymerized to form a thin organic polymer layer. After this pre-emulsion polymerization (step A), the post-emulsion polymerization (step B) was continued to obtain the NCE, which could readily form highly transparent hybrid films by casting even at a silica content higher than 50 wt.%. These hybrid films showed a variety of intriguing properties such as anti-soiling and stain-resistant properties that are necessary for their use as high-quality wall paints [11,12,14]. However, the above recipe for preparing NCEs is rather complex, sometimes causing gelation during the post-emulsion polymerization or in the paint formulation. Therefore, a much simpler recipe for manipulating silica nanoparticles is needed for preparing a water-borne hybrid emulsion.

With the above recipe re-examined, it is evident that the colloidal silica particles obtained after the pre-emulsion polymerization must have a very thin polyacrylate coat (< 5 nm in thickness) [14] and ought to be so well stabilized as to prevent particle aggregation. The author therefore thinks it possible to directly incorporate these surface-coated colloidal silica particles into the ordinary acrylic emulsions to achieve the hybridization of silica and polyacrylate polymers (steps A and C in Scheme 1). In this study, the surface-coated colloidal silica particles (PreEm) obtained in the pre-emulsion step were mixed with general acrylic emulsions (AcEm) to investigate the hybridization effect on the morphology and

properties of the mixed emulsions (PreEm/AcEm) and the hybrid films prepared from them. Then, the PreEm/AcEm is totally characterized in comparison with the corresponding NCEs in which the silica particles are covered with a thicker polyacrylate coat.

## EXPERIMENTAL

### Materials

Colloidal silica, ADELITE® AT-50 (abbreviated as CS-50), was supplied by ADEKA Corp. (Tokyo, Japan). Its silica content was 50 wt%, and the average diameter of the colloidal silica particles was in a range of 20-30 nm. A nonionic surfactant, ADEKA REASOAP® NE-10 (poly(ethylene glycol) mono-[1-(allyloxy)-3-(4-nonylphenoxy)-2-propyl] ether, abbreviated as NIS), was also supplied by ADEKA Corp. Its chemical structure is shown in Figure 1(a). The degree of polymerization (*n)* of its poly(oxyethylene) chain was 10, and its $T_{cp}$ was reported to be 40 °C. Non-reactive (PELEX® SS-H) and reactive anionic surfactants (HITENOL® KH-10) were supplied by Kao Corp. (Tokyo, Japan) and DKS Co. Ltd. (Kyoto, Japan), respectively. Their chemical structures are shown in Figure 1. Potassium peroxydisulfate (KPS), butyl acrylate (n-BA), methyl methacrylate (MMA), methacrylic acid (MAA), and other chemicals were of industrial grade and used as received.

### Measurements

Scanning electron microscopy (SEM) was performed on a VE-7800 electron microscope (KEYENCE Corp., Osaka, Japan) operated at 10 kV. Samples were gold-coated on an aluminum stage prior to observation. Scanning transmission electron microscopy

(STEM) was conducted on a HD-2700 electron microscope (Hitachi High Technologies Corp., Tokyo, Japan) with an accelerating voltage of 200 kV. A diluted sample of an emulsion was cast on a Cu mesh of 150 μm in grid pitch (Okenshoji Co., Ltd., Tokyo, Japan) and dried in vacuum before the measurement. Dynamic light scattering (DLS) was measured on a Photal® ELS-8000 instrument (Otsuka Electronics, Hirakata, Osaka, Japan) by utilizing a He/Ne laser (632.8 nm) at 25 °C. The scattering angle was fixed at 90 °. The data were analyzed according to cumulant method, and their reproducibility was confirmed with at least three experiments. Fourier transform infrared spectroscopy (FT-IR) was conducted on a Spectrum® GX spectrophotometer (Perkin Elmer, USA) with a KBr/sample pellet form from 4000 to 450 $cm^{-1}$ with a resolution of 4 $cm^{-1}$. Atomic force microscopy (AFM) was conducted in dynamic force mode (tapping mode) using a SPM-9700 scanning probe microscope (SHIMADZU Corp., Kyoto, Japan). A commercially available silicon tip with a spring constant of 25-35 N/m and a single beam cantilever of 125 μm long was used in a resonance frequency range from 260 to 410 kHz.

**Preparation of colloidal silica bearing thin polyacrylate coat (PreEm)**

By slight modification of the previously reported method [11], two PreEm samples, PreEm-1 and PreEm-2, were prepared. Typically, an aqueous solution (50 mL) of NIS (10.0 g) was dissolved in a CS-50 (400 g) at 40 °C, and the temperature of the mixture was raised to 70 °C with stirring. The mixture was continuously stirred at 70 °C for 1 h in a nitrogen atmosphere. To this mixture, a portion (10.0 g) of a monomer mixture of MMA, n-BA, and MAA (MMA: *n*-BA: MAA= 34.5/65.0/0.5 in wt%: soft composition) was added, and its polymerization was started by adding an aqueous solution (20 mL) of KPS (0.55 g). The whole mixture was stirred at 70 °C for 2 h for completing the polymerization and cooled down to room temperature to obtain a sample of PreEm-1, which consisted of colloidal silica

particles covered with a soft polyacrylate showing a glass transition temperature ($T_g$) of -16 °C. The solid content of PreEm-1 was 44.5 wt% with a silica/polyacylate (Si/Ac) ratio of 200/ 10 (wt/wt-%). By the same process, PreEm-2 consisting of colloidal silica particles covered with a harder polyacrylate was also prepared by changing the monomer composition to MMA: *n*-BA: MAA= 53.3/46.3/0.4 in wt%. The $T_g$ of this polyacrylate was 10.0 °C, and the solid content and Si/Ac ratio were identical to those of PreEm-1.

**Preparation of NCE and AcEm**

Both nanocomposite emulsion samples of NCE-1 and NCE-2, which consisted of the above soft and hard polyacrylates, respectively, were prepared by following the method previously reported [11]. Typically, an aqueous solution (145 g water) of KPS (0.55 g) and NIS (10.0 g) was added dropwise into an CS-50 (400 g) under vigorous stirring in a nitrogen atmosphere at 40 °C. The temperature of the mixture was raised to 70 °C, and a portion (10.0 g) of a monomer mixture (200 g) of MMA, n-BA, and MAA was dropwise added to the mixture. The stirring of this mixture was continued at 70 °C for 1 h to finalize the polymerization. In the following step, an aqueous mixture (56 g water) of KPS (0.65 g) and PELEX® SS-H (14 g) was added, and the rest of monomer mixture (190g) was dropwise added in 3 h. The reaction mixture was kept stirring at 70 °C for an additional hour to complete the polymerization. Finally, the mixture was cooled down to room temperature and added with an aqueous ammonium solution (25 wt %, 3.6 g amount) for controlling its pH to 9-10 to obtain a sample of NCE-1. The solid content of the NCE-1 was about 50 wt% with a Si/Ac ratio of 200/200 (wt/wt-%). Similarly, an NCE-2 sample consisting of a polyacrylate of MMA: *n*-BA: MAA= 53.3/46.3/0.4 ($T_g$= 10.0 °C) was also prepared.

Two acrylic emulsions (AcEm-1 and AcEm-2 consisting of the soft and hard polyacrylates, respectively) were prepared by the ordinary emulsion polymerization of the

monomer mixtures of MMA, *n*-BA, and MAA by utilizing a reactive anionic surfactant HITENOL® KH-10 (1.26wt%). Their monomer compositions were MMA: *n*-BA: MAA= 34.5/65.0/0.5 (AcEm-1: $T_g$= -16 °C) and 53.3/46.3/0.4 (AcEm-2: $T_g$= 10.0 °C) in wt%, respectively. Their solid content was identical (47.3 wt%) to the above.

**Preparation of mixed emulsions and their film formation**

The PreEm and AcEm comprising the identical polyacrylate were mixed in different ratios to obtain hybrid emulsions having certain Si/Ac ratios: 100/100, 150/100, and 200/100. Then, the solid content of the mixed emulsion was finally adjusted to about 45 wt%. Mixed emulsions of CS-50 and AcEm were also prepared likewise as controls. Each of the mixed emulsions obtained was cast on a glass plate by using an applicator forming a liquid film of 150 μm in thickness and air-dried overnight to obtain a hybrid film of silica/polyacrylate.

**Sample preparation for analyses**

For the STEM analysis, a portion of PreEm-1 obtained above was dialyzed against deionized water with a regenerated cellulose membrane (Spectrum® /Por 6, a product of Spectrum Laboratories, Inc., USA and sold by Ieda Trading Corp., Tokyo, Japan) having a cut-off molecular weight over 50 kDa (the average pore size: 6-7 nm in diameter). The dialysis was continued for 1 week with the external deionized water renewed every half day. Then, a small portion of the dialyzed sample was filtered through a STEM micron grid Cu mesh (grid pitch = 150 μm, Okenshoji Co., Ltd., Tokyo, Japan) and subjected to the STEM measurement. Another portion of the dialyzed sample was dried up in air (30 °C) and thoroughly dried in vacuum at room temperature for 1 day. The residue was subjected to the FT-IR analysis.

For the film hardness test, each emulsion was cast on a tin plate with an applicator

mentioned above. The resultant liquid film was solidified in air and thoroughly dried in a hot-air drier at 100 °C for 1 h. The coating film thus prepared was subjected to scratch hardness test according to JIS K 5600-5-4, which was based on the ordinary pencil method.

For obtaining a self-supported film, each emulsion was cast on a polyethylene plate with an applicator mentioned above. The cast film was first solidified in air and thoroughly dried at 100 °C for 1 h. The dried film was easily separated from the substrate.

## RESULTS

### Colloidal particles bearing thin polyacrylate coat

An aqueous solution of NIS, a nonionic surfactant with $T_{cp}$ = 40 °C, undergoes clouding above 40 °C by its thermal dehydration. When this clouding was induced in the presence of colloidal silica particles CS-50, the dehydrated NIS molecules were allowed to deposit on the colloidal silica surface to give a clear colloidal system as reported previously [14]. To this colloidal system, a small amount of an acrylic monomer mixture (MMA: *n*-BA: MAA= 34.5/65.0/0.5 in wt%) was added and polymerized to obtain a PreEm-1 consisting of silica particles coated with a soft polyacrylate ($T_g$= -16 °C, silica/NIS/Acryl = 34.7/1.02/1.02 in wt/wt/wt). Figure 2 compares the size distribution curves of CS-50 (a) and PreEm-1 (b) as measured by DLS. It is noted that the average diameter (57.9 nm) of the colloidal particles of PreEm-1 became slightly larger than that (46.3 nm) of the original silica particles without much change in size distribution (see Run no. 1 and 2 in Table 1). The increase in diameter of about 10 nm is attributed to the shell formation in the surface of colloidal silica particles.

Figure 3 shows the morphologies of colloidal particles of PreEm-1 cast on a silicon wafer surface. The SEM photo (Figure 3a) indicated that the colloidal particles formed an agglomeration state by covering the substrate surface. Their microscopic state of

agglomeration was clearly shown by the AFM image in lower magnification (Figure 3b) where the particles formed clusters of different sizes. The AFM image at higher magnification (Figure 3c) revealed a nanometer-size morphology of the particles, although the presence of polymer shell could not be well identified on the particle surface. The diameters of the particles ranged from 30 nm to 70 nm, being comparable to the above average diameter determined by DLS.

Figures 4 and 5 show the typical STEM photos of the original colloidal silica particles (CS-50: control) and those of the colloidal particles sampled from the NIS-deposited CS-50 (CS-50/NIS) and PreEm-1. Compared with the original colloidal silica particles (Figure 4) the particle surface became significantly smoother and less connected with each other in CS-50/NIS and PreEm-1. Further comparison of the both SEM figures of CS-50/NIS (Figure 5(a)) and PreEm-1 (Figure 5(c)) revealed that the latter particles have smoother surface than the former ones. In the former case, the surface retained the dot matrix even with NIS deposits (see the expanded SEM image of Figure 5(a)), while in the latter the dot matrix became denser and flatter (see the expanded image in Figure 5(c)). The STEM photo of CS-50/NIS in lower magnification showed interfacial spaces between the particles as shown by an arrow in Figure 5(b), supporting the existence of NIS deposits. The STEM photo of PreEm-1 (Figure 5(d)) also showed similar interfacial spaces which ought to have been formed by the presence of polyacrylate coat layers on the particles. More clearly, an expanded STEM image of the particles of PreEm-1 (the inlet image of Figure 5(d)) revealed a resinous coat layer (in brighter contrast) covering the surface of each silica particle (in dark contrast). This skin layer was shown to have a thickness of about 1-3 nm. This value was slightly lower than that estimated from the above DLS results that the increase in the particle size of PreEm-1 was almost 10 nm. This difference is attributed to the drying and hydration states of the surfactant-containing layer in the STEM and DLS measurement, respectively. It

is therefore evident that the acrylic monomer was polymerized around the surface deposits of NIS to cover each of the colloidal silica particles in a form of polymer skin. This thin polymer coat can work not only as the blocker for particle coagulation but also as the site of the next post-emulsion polymerization to produce the NCE.

The IR spectra of the particles isolated from a series of colloidal systems are compared in Figure 6. The particles from the CS-50/NIS (Figure 6(b)) showed a spectrum similar to that of the original silica particles (Figure 6(a)), probably because of the absence of IR absorption of NIS in the wave length region measured. On the other hand, the particles from PreEm-1, which was prepared in the presence of NIS (Figure 6(d)), exhibited a weak absorption at 1736 $cm^{-1}$ due to the polyacrylate carbonyl stretching, whereas those from the corresponding pre-emulsion system prepared in the absence of NIS (Figure 6(c)) showed no carbonyl absorption. This result indicated that the polyacrylate coat had been formed only in the presence of surface deposits of NIS, supporting the function of NIS in mediating the polymerization on the colloidal silica surface.

The preEm-1 prepared above consisted of a soft polyacrylate ($T_g$= -16 °C) having a considerably lower MMA composition (MMA/*n*-BA = 34.5/65.0). This composition had formerly been optimized for manufacturing an NCE-based wall paint [12.14], and accordingly the same composition was mainly examined in the present study. However, it became evident that a harder polyacrylate was more favorable for obtaining a coating film having solid surface (vide infra), and another PreEm-2 consisting of colloidal silica particles covered with a harder polyacrylate was prepared. This polyacrylate had an MMA-rich composition (MMA: *n*-BA: MAA= 53.3/46.3/0.4) and showed a higher $T_g$ value (= 10.0 °C). The nano-composite structure of the resultant PreEm-2 was considered to be identical with that of PreEm-1.

**Mixed emulsions of PreEm and AcEm**

Both PreEm-1 and PreEm-2 obtained above were respectively mixed with the ordinary acrylic emulsions AcEm-1 and AcEm-2 comprising similar monomer composition to obtain mixed emulsions (PreEm-1/ AcEm-1 and PreEm-2/ AcEm-2). The mixing was done by adjusting the Si/ Ac ratios to 100/100, 150/100, and 200/100 in wt/wt-% at an identical solid content of about 45 wt%. Figure 7 shows the size distribution curves of the colloidal particles in the mixed emulsions prepared with AcEm-1 at a Si/Ac ratio of 150/100 as measured by DLS. Evidently, the colloidal size distribution curves of both the mixed emulsions CS-50/ AcEm-1 (b) and PreEm-1/ AcEm-1 (c) were almost identical with the curve of the acrylic emulsion AcEm-1 (a). They were in sharp contrast to the curve of the NCE-1 (Si/Ac= 150/100) showing a broad size distribution ranging from 20 nm to 400 nm in particle diameter. Since the average particle size of AcEm-1 (110 nm in diameter) was much larger than that of CS-50 (46 nm) or PreEm-1 (58 nm), the light scattering from the smaller particles ought to have become much weaker than that from the larger particles and hidden behind the latter. It was however confirmed that when the amount of CS-50 and PreEm-1 added to AcEm-1 was tripled the size distribution curve broadened toward the smaller diameter region. This result indicated that the particles of both CS-50 and PreEm-1 were independently dispersed in AcEm-1 and that the interaction between the colloidal particles of PreEm-1 and AcEm-1 was as weak as that between the colloidal particles of CS-50 and AcEm-1. If any interaction would have been present between these particles in the mixed emulsions, the average particle size should have become larger or non-unimodal. The author thinks that the particle interaction between CS-50 and AcEm-1 or between PreEm-1 and AcEm-1 ought to be repulsive because they have negative surface charge. Table 1 summarizes the sizes and dispersities of the colloidal particles of the mixed emulsions as determined by DLS. It was indicated that the particle dispersity broadened with increasing the Si/Ac ratio without much

change in their average diameter. The dispersity became significantly larger in PreEm-1/ AcEm-1 than in CS-50/ AcEm-1, suggesting a slightly stronger particle interaction in the former.

**Coating films of the mixed emulsions**

Each of the mixed emulsions CS-50/ AcEm-1 and PreEm-1/ AcEm-1 as well as NCE-1 (control) (for which the component polymer was a polyacrylate showing $T_g$= -16 °C) was cast on a glass plate to form a coating film. Figure 8 shows the photos of the coating films obtained after drying at ambient conditions. In the case of PreEm-1/ AcEm-1, the coating film retained transparent state at a Si/Ac ratio lower than 150/100, whereas in CS-50/ AcEm-1 a transparent film was obtained only at a Si/Ac ratio of 100/100. Since NCE-1 gave transparent films at an even higher Si/Ac ratio of 200/100, the mixed emulsion PreEm-1/ AcEm-1 was shown to be in a middle position in terms of retention of transparency of the coating films among the three emulsion systems. The loss of transparency could be attributable to agglomeration of silica particles during the drying of emulsion films, and the use of PreEm-1 was shown to be effective for retarding the particle agglomeration in the film formation of the hybrid emulsion.

Figure 9 shows the SEM photos of the film surfaces of the CS-50/ AcEm-1, PreEm-1/ AcEm-1 and NCE-1 whose Si/Ac was identical (150/100). Similar particle aggregation states were observed in the three film samples, although the pits and grooves formed in the surfaces became smaller in the order of CS-50/ AcEm-1 > PreEm-1/ AcEm-1 > NCE-1. Since in the three systems an identical soft polyacrylate having $T_g$ = -16 °C was used, the soft (rubbery) polymer layer was likely to migrate from the top to the bottom area of the silica particles when dried, forming a nodulous surface with leaving the agglomerated silica particles. Such a tendency was observed even in the case of NCE-1 having a thick coat layer

around each silica particle, although the particle agglomeration became more homogeneous.

Figure 10 shows typical AFM images of the same emulsion films formed on a silicon wafer surface. It was confirmed that the single emulsion AcEm-1 formed a flat surface with a small number of shallow pits (4.07 nm in depth, Figure 10(a)). On the other hand, the two mixed emulsions and NCE-1 exhibited granular morphologies with undulation (130-240 nm in height) and formation of many pits shown in dark color. In the CS-50/ AcEm-1 (Figure 10(b)), the surface was covered with agglomerated silica particles, probably because the matrix polymer had migrated beneath the particles. In fact, the AFM images in phase mode (Figure 11) displayed a morphology of polymer layer sinking beneath the particles. More interestingly, the enlarged image in the inlet of Figure 10(b) exhibited a morphology in which many particles surround a pit shown in dark color. Even the NCE-1 film (Figure 10(d)) indicated the similar granular morphology, although it was more homogeneous. The enlarged inlet image of Figure 10(d) exhibited a morphology of particles aggregating around a pit. The respective particles here showed a skewed shape probably because some part of their thick polyacrylate coat had migrated beneath the silica particles. Different from these emulsion films, the mixed emulsion film of PreEm-1/ AcEm-1 exhibited a well-dispersed particle morphology (Figure 10(c)), although the undulation was the largest. As noted in the enlarged inlet image of Figure 10(c), many particles seemed to float in the polyacrylate matrix of AcEm-1 without aggregation. The deep pits shown in Figure 10(c) may have been formed by the migration of the soft matrix having few particles inside. This interesting morphology was reasonably attributed to the strong surface interaction between the PreEm particles and AcEm particles. Close look into Figure 10(c) in lower magnification (background) revealed that the PreEm particles were partly accumulating in ball shape. This accumulation of PreEm particles around an AcEm particle is similar to the formation process of a Pickering emulsion although in the present case it has been induced during the drying of

the emulsion film. Since no size change was observed between the mixed and single emulsions as described above (Table 1), the interaction of the AcEm-1 and PreEm-1 particles was not strong in the state of emulsion. Their interaction should have been increased with the loss of aqueous medium to make the AcEm particles aggregate around the PreEm particles. In the CS-50/ AcEm-1, in return, such surface interaction was absent even in the drying process, and silica particles were separated from the polymer matrix to undergo macro-size aggregation, causing the loss of transparency. In NCE-1, the particle aggregation was also induced, but it was enough homogeneous to form few macro-size aggregates. Based on these findings, the combined use of AcEm and PreEm bearing thin polyacrylate coat is advantageous for homogeneously distributing silica nanoparticles in cast films of polyacrylate emulsions as the single use of NCE having thick polyacrylate coat. Since the PreEm can be more easily prepared than NCE and mixed with various types of pre-made acrylic emulsions with a wider variety of monomer compositions than NCE, the structure and property control of the hybrid emulsion films can be accomplished with the PreEm/AcEm mixing method.

Similar coating films were obtained from the mixed emulsions CS-50/ AcEm-2 and PreEm-2/ AcEm-2 as well as from the NCE-2 emulsion which consisted of a polyacrylate with a harder monomer composition ($T_g$= 10 °C). Typical photos of the coating films prepared from the three emulsions at a Si/Ac ratio of 150/100 are compared in Figure 12. The films of PreEm-2/ AcEm-2 and NCE-2 retained almost transparent state, whereas the film of CS-50/ AcEm-2 became completely translucent. This relation was similar to that observed in the aforementioned films of CS-50/ AcEm-1, PreEm-1/ AcEm-1, and NCE-1. These data strongly supported that PreEm-1 and PreEm-2 consisting of silica nanoparticles with thin polyacrylate coats of different monomer compositions can be used as inorganic modifiers of acrylic emulsions and other related matrix polymers.

**Properties of coating films**

The coating films obtained above were subjected to pencil hardness test. Table 2 compares the scratch hardnesses of the coating films prepared from the emulsions of AcEm-2 series (CS-50/ AcEm-2, PreEm/ AcEm-2, and NCE-2). Since the coating films of the other AcEm-1 series (CS-50/ AcEm-1, PreEm-1/ AcEm-1 and NCE-1) were too soft, their hardness could not be measured. The coating film of the original AcEm-2 showed a scratch hardness of 2B, being still soft. By incorporation of colloidal silica particles (CS-50/ AcEm-2 film), in return, the scratch hardness increased to H at a Si/Ac ratio of 150/ 100. However, the hardness declined to the original level of 2B at a Si/Ac ratio of 200/ 100 where the agglomeration of silica particles was obvious. On the other hand, the films of PreEm-2/ AcEm-2 exhibited increased hardnesses of HB and 2H at Si/Ac ratios of 100/100 and 150/100, respectively. At a higher Si/Ac ratio of 200/100, the hardness deceased to HB because of the increased agglomeration of the PreEm particles. In the case of NCE-2, the film hardness was not much improved with increasing the silica content, because the surface was always covered with slightly thick polymer layers. These data supported the availability of PreEm-2 in tuning the film hardness of acrylic emulsions.

The coating films prepared on glass plates were hardly peeled off from the substrates, being difficult to make self-supported polymer films. So, we cast the colloidal solutions on polyethylene plates to fabricate their polymer films. The colloidal solutions from which self-supported films could be obtained are shown by character F in Table 3. It was confirmed that at Si/Ac=100/100 every mixed emulsion as well as NCE gave hybrid films whereas at higher silica content of Si/Ac=150/100 both mixed emulsions with CS-50 gave brittle films that could not be peeled off. On the other hand, the mixed emulsions with PreEm-1 and PreEm-2 gave self-supported films at Si/Ac=150/100. Even at Si/Ac=200/100,

a brittle film could be obtained from PreEm-2/ AcEm-2. These data also demonstrated the effectiveness of PreEm in controlling the properties of silica-acryl hybrid films.

## DISCUSSION

As mentioned in Introduction, miniemulsion polymerization has been believed to be the most efficient method for incorporating inorganic nanoparticles into a polymer matrix of nanoscale [4-6]. In this method, an alkane/monomer mixture is dispersed in an aqueous medium to make organic droplets of c.a., 50 to 500 nm in diameter, and into which nanoparticles are suitably included. For efficient inclusion of nanoparticles, the compatibility of the inorganic particles with the organic phase (monomer) must be improved by surface modification of the particles. In the case of silica nanoparticles, the modification can be accomplished by surface reaction with such organic silane agents as 3-(trimethoxysilyl)propyl methacrylate (MPS) [17-20] and (γ-glycidoxypropyl) trimethoxysilane (GPTMS) [21,22]. The resultant silica nanoparticles having modified surface can efficiently be distributed to the organic phase including acrylic monomers and encapsulated by the following polymerization [23]. Such surface modification is also possible by simple adsorption of cationic surfactants such as hexadecyltrimethylammonium bromide [24,25] or cationic initiators [26] on the anionically charged silica surface. In the latter case, the polymerization is initiated from the adsorption site to generate a polymer layer on the silica surface. Addition of cationic monomers such as 4-vinylpyridine has also been effective for inducing the surface polymerization for coating [27]. Aliphatic carboxylic acids such as oleic acid is known to work as surface modifiers of colloidal silica particles [7]. Living and controlled radical polymerization (L/CRP) such as reversible addition–fragmentation chain transfer (RAFT) polymerization [28-30] and atom transfer

radical polymerization (ATRP) [31] can be conducted for obtaining hybrid nanoparticles consisting of polymers with controlled molecular weight. Raspberry-like hybrid nanoparticles are also prepared by Pickering-type miniemulsion polymerization [32] as well as by competitive polymerization of vinyl monomers and inorganic precursors [33]. In these emulsion systems, however, control of the encapsulation is not so easy, making the emulsion stability unfavorably lower [8]. Furthermore, emulsification must be done by sonication or high-pressure homogenization for providing the mini-droplet state [34]. In contrast to these mini-emulsion processes, our NCE process is much simpler in terms of emulsification and polymerization methods [25].

In this study, it has clearly been demonstrated that NIS can effectively deposit on the surface of colloidal silica particles by its clouding behavior and aid acrylic monomers to settle around the silica particles and generate a thin polymer coat on the particle surface by the following polymerization. Probably, the allyl group of NIS is copolymerized during the polymerization of acrylic monomers, and the NIS moieties ought to be firmly immobilized in the surface coat layer. The presence of the thin polyacrylate coat on the colloidal silica particles was directly observed by the STEM analysis of PreEm-1 (Figure 5). Thus, the resultant colloidal silica particles covered with thin polyacrylate coat (PreEm particles) can function not only as the cores for the further emulsion polymerization to produce NCE, but also as inorganic modifiers of the ordinary acrylic emulsions. Here, these PreEm particles were successfully incorporated into the ordinary acrylic emulsions (AcEm) to obtain their mixed emulsions that can give hybrid-type coating films. Although the polyacrylate coat of the PreEm had identical monomer compositions with the AcEm particles, the interaction between PreEm and AcEm particles is not so strong in the mixed emulsion state, and both particles are likely to preserve their own particulate morphologies as in the case of the mixed emulsion of CS-50/ AcEm. Probably, the surface tension of both the anionically charged

particles are too strong to heterogeneously surface-agglomerate as the Pickering emulsions. However, with progress of drying of the mixed emulsions, the smaller PreEm particles gradually gather around the larger AcEm particles and surround them. In this stage, the inter-particle interaction among the PreEm particles is not so strong as to undergo aggregation, and the PreEm particles can distribute inside the AcEm particles by the polymer-polymer interaction between the PreEm and AcEm particles. In the alternative CS-50/ AcEm system, the naked silica particles are incompatible with the polymer surface of AcEm particles, and they readily aggregate with each other in the periphery of AcEm particles. Even in the case of NCE having a broader size distribution, the smaller particles are likely to gather and come into close contact with each other, resulting in inhomogeneous distribution and partial aggregation of the core particles in place to place by migration of thick, soft polymer coat. This partial aggregation occurring in the NCE film is different from the aggregation mode of PreEm particles buried in acrylic polymer matrix and completely different from the aggregation observed in the CS-50/ AcEm film that is likely to lose transparency. It was also confirmed that the PreEm-2/ AcEm-2 mixed emulsions gave cast films having harder surface than NCE-2 and CS-50/ AcEm-2. This fact may be because the silica nanoparticles have been distributed more homogeneously in the cast films of PreEm/ AcEm-2 and became enriched in the film surface. When silica nanoparticles are agglomerated as in the case of CS-50/ AcEm-2, the soft polymer domain is exposed to the top surface to lower the hardness. In the case of NCE-2, the slightly thick polymer coat formed around the silica nanoparticles may likely remain the top surface of the cast films, resulting in the lower hardness. Since in the PreEm-1/ AcEm-1 both the coating and matrix polymers is too soft, the silica particles are not well fixed on the film surface to less resist against friction, making it difficult to obtain a hard surface by using modified silica nanoparticles. Even in the case of PreEm-2/ AcEm-2 consisting of a polyacrylate showing $T_g$= 10.0 °C is rubbery at room temperature, it may not

produce enough hard surface (2H at the highest). Much higher MMA composition ought to be adopted for obtaining a hard coating surface. We will report on it in the future. Consequently, the PreEm having a single-modal size distribution ought to show high dispersing ability in AcEm and have high potential as a versatile inorganic particle modifier of acrylic emulsions and their coating films.

## CONCLUSION

In this study, the author examined the mixing effect of the colloidal silica particles having a thin polyacrylate coat (5 wt % amount relative to colloidal silica: PreEm) on the ordinary acrylic emulsions (AcEm) as well as on the morphology and properties of the coating films prepared from the mixed emulsions (PreEm/AcEm). The PreEm emulsions were readily prepared with the aid of a nonionic surfactant NIS showing a low $T_{cp}$ of 40 °C. It was confirmed that this nonionic surfactant first deposited on the surface of colloidal silica particles above its $T_{cp}$ to provide the sites for surface adsorption and the following polymerization of acrylic monomers. The presence of very thin polyacrylate coat (< 10 nm in thickness) on the silica nano-particles was successfully verified by STEM analyses. These surface-coated colloidal silica particles of PreEm were readily incorporated into the ordinary AcEm to obtain silica/ polyacrylate hybrid emulsions. The colloidal size distribution curves of the mixed emulsions AcEm/ PreEm were almost identical with the curves of the AcEm itself and a mixed emulsion CS-50/ AcEm, being in sharp contrast to the curve of the NCE showing a broad size distribution ranging from 20 nm to 400 nm in particle diameter. It was therefore indicated that the interaction between the colloidal particles of AcEm and PreEm was as weak as that between AcEm and CS-50.

The mixed emulsion AcEm-1/ PreEm-1 (with a soft polymer composition) could form

transparent coating films at a Si/Ac ratio below 150/100 in which the colloidal particles were distributed in the matrix polymer without aggregation. This morphology was different from that of the films obtained from the CS-50/ AcEm-1 and NCE-1 in which the silica particles were agglomerated in the polymer matrix to a greater or lesser extent, respectively. The films of PreEm-2/ AcEm-2 (with a harder polymer composition) exhibited increased hardness with increasing the silica content to 150 % but decreased at the higher content of 200 % where the particle agglomeration became evident. This increase in hardness was significantly greater than that with CS-50/ AcEm-2 or NCE-2, supporting the availability of PreEm-2 in tuning the film hardness of acrylic emulsions. These data clearly supported the characteristic nature of PreEm in hybridization of colloidal silica and acrylic emulsions with which the structure and properties of the resultant acryl-silica hybrid films can be controlled.

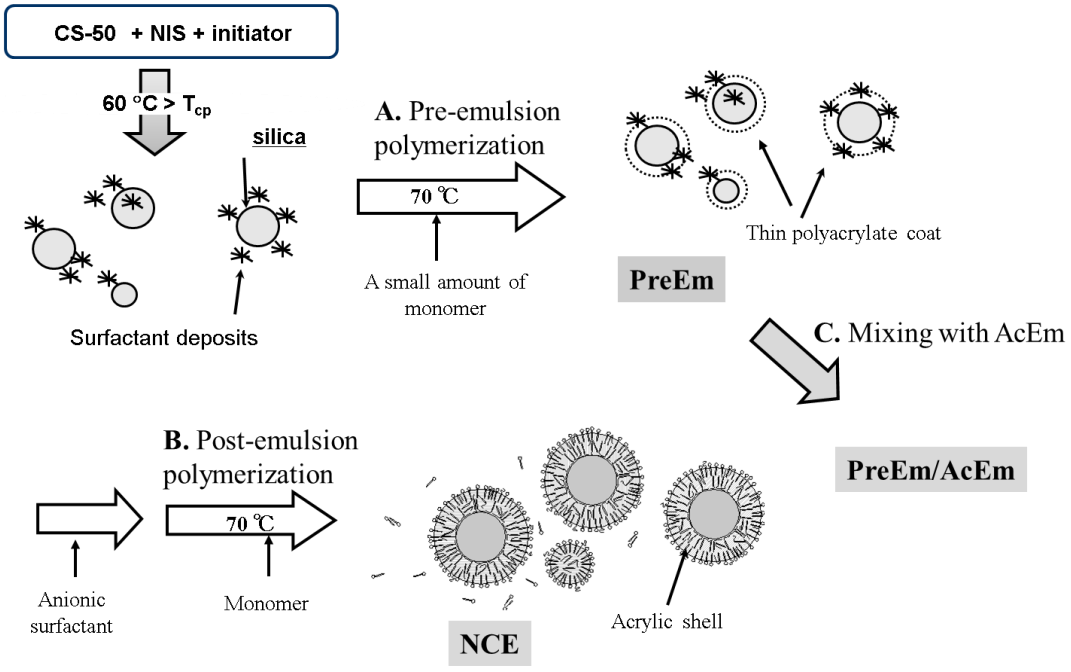


**Scheme 1. Synthetic routes to NCE (steps A and B) and hybrid emulsions (steps A and C)**

**Table 1. Size and size distribution[1)] of the colloidal particles of different colloidal solutions[2)] as measured by DLS.**

| Run No. | Colloidal solution (Si/ Ac) | Average diameter (nm) | Dispersity ($10^{-2}$) |
|---|---|---|---|
| 1 | CS-50 (100/0) | 46.3 | 8.36 |
| 2 | PreEm-1 (100/5) | 57.9 | 12.3 |
| 3 | AcEm-1 | 113 | 4.49 |
| 4 | CS-50/ AcEm-1 (100/100) | 111 | 0.445 |
| 5 | CS-50/ AcEm-1 (150/100) | 108 | 2.30 |
| 6 | CS-50/ AcEm-1 (200/100) | 108 | 2.89 |
| 7 | PreEm-1/ AcEm-1 (100/100) | 112 | 3.29 |
| 8 | PreEm-1/ AcEm-1 (150/100) | 105 | 8.27 |
| 9 | PreEm-1/ AcEm-1 (200/100) | 106 | 7.53 |
| 10 | NCE-1 (100/100) | 63.1 | 14.6 |
| 11 | NCE-1 (150/100) | 75.1 | 20.7 |
| 12 | NCE-1 (200/100) | 124 | 28.2 |

**1) Determined by cumulant method.**

**2) With an identical solid content of 45 wt%.**

**Table 2. Scratch hardnesses of the coating films of various colloidal solutions.** [1)]

| Colloidal solution (Si/Ac) | Scratch hardness | Film thickness (μm) |
|---|---|---|
| AcEm-2 | 2B | 25.7 |
| CS-50/ AcEm-2 (100/100) | F | 29.0 |
| CS-50/ AcEm-2 (150/100) | H | 27.3 |
| CS-50/ AcEm-2 (200/100) | 2B | 26.3 |
| PreEm-2/ AcEm-2 (100/100) | HB | 21.3 |
| PreEm-2/ AcEm-2 (150/100) | 2H | 19.3 |
| PreEm-2/ AcEm-2 (200/100) | HB | 21.3 |
| NCE-2 (100/100) | HB | 27.0 |
| NCE-2 (150/100) | HB | 26.7 |
| NCE-2 (200/100) | F | 25.7 |

**1) Measured by the pencil method according to JIS K 5600-5-4.**

**Table 3. Fabrication of self-supported films from the colloidal emulsions[1)].**

| Si/Ac | 100/100 | 150/100 | 100/200 |
|---|---|---|---|
| CS-50/AcEm-1 | F | | |
| PreEm-1/AcEm-1 | F | F | |
| NCE-1 | F | F | |
| CS-50/AcEm-2 | F | | |
| PreEm-2/AcEm-2 | F | F | (F) |
| NCE-2 | F | F | |

**1) A self-supported film was fabricated from AcEm-2 ($T_g$= 10 °C), whereas no film could be obtained from AcEm-1 ($T_g$= -16 °C).**

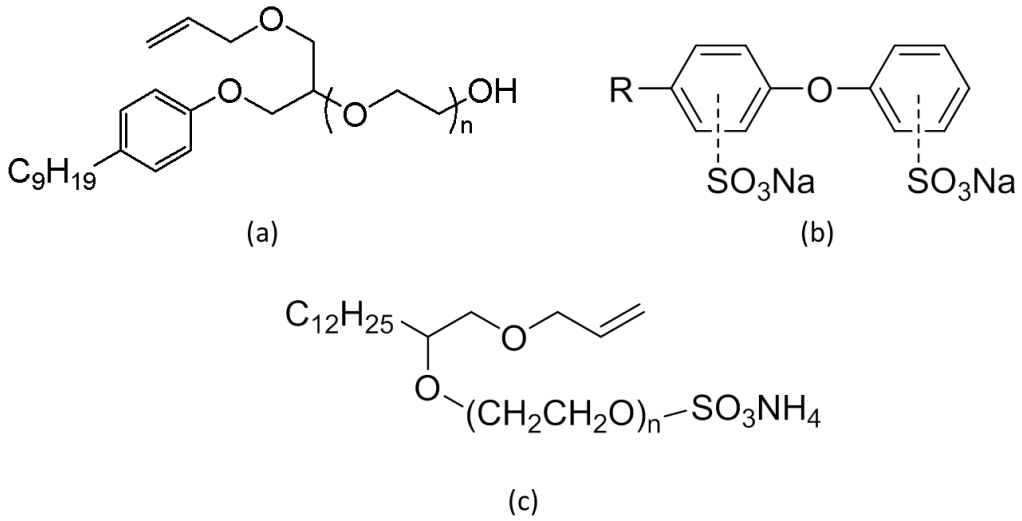


**Figure 1. Chemical structures of (a) NIS (ADEKA REASOAP® NE-10 (*n*=10)), (b) PELEX® SS-H, and (c) HITENOL® KH-10 (*n*>10).**

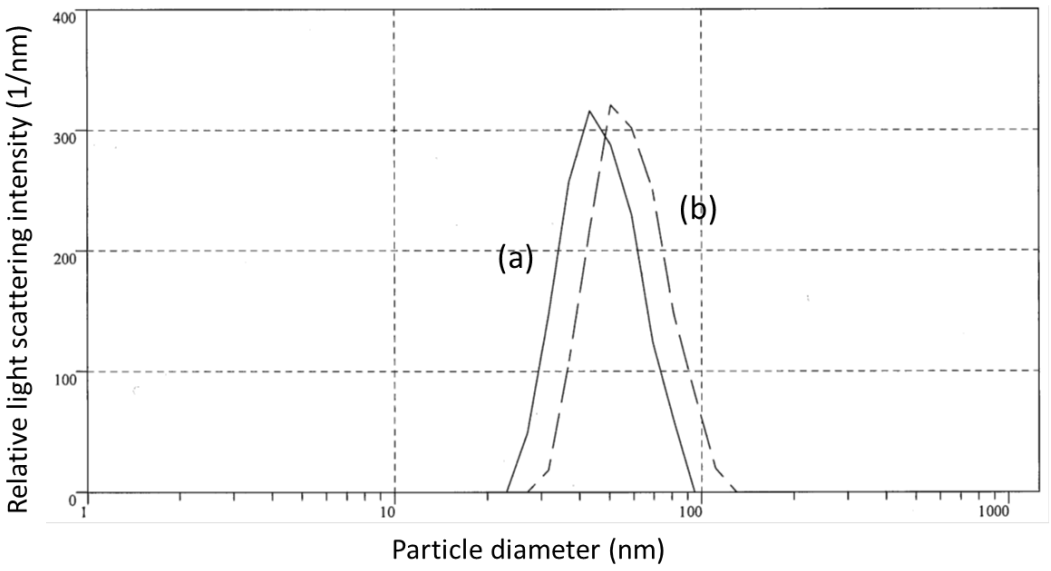


**Figure 2. Size distribution curves of the colloidal particles of (a) CS-50 (solid line), (b) PreEm-1 (dashed line) as measured by DLS.**

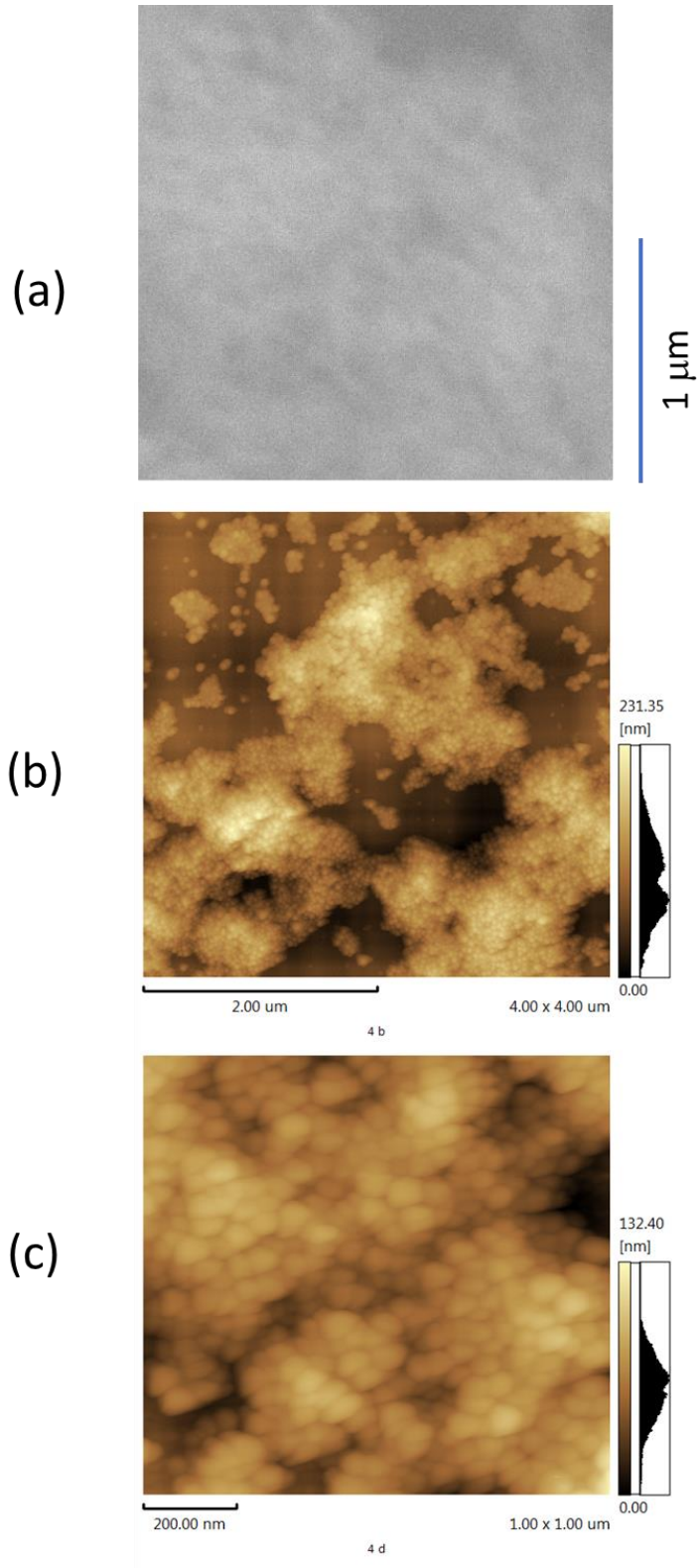


**Figure 3. (a) A typical SEM micrograph and AFM images of PreEm-1 cast on a silicon wafer in (b) low and (c) high magnifications.**

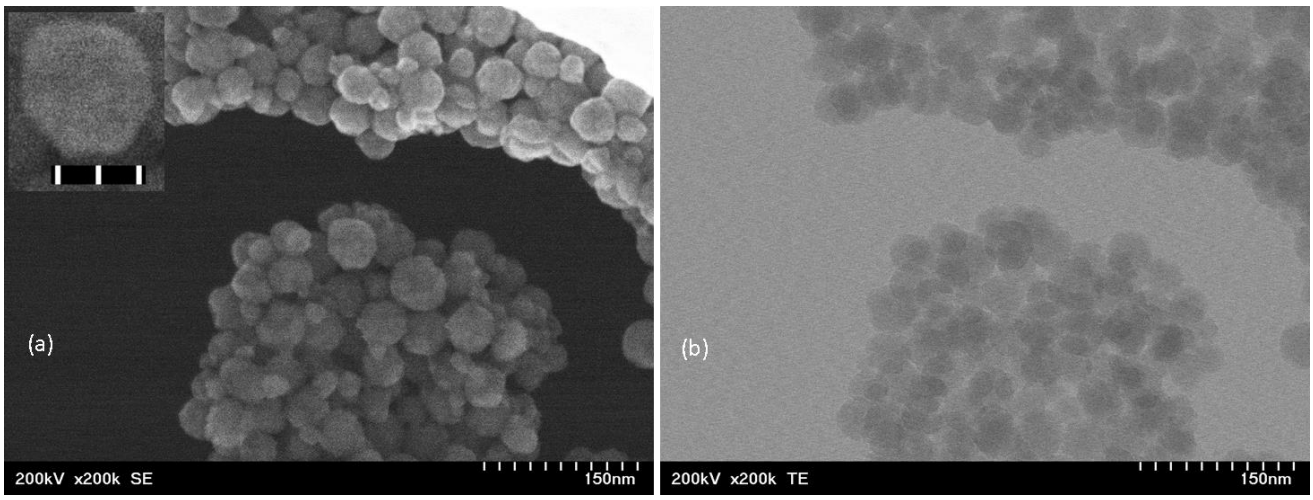


**Figure 4. Typical SEM (a) and STEM (b) images of the original colloidal silica (CS-50) . The dot bar in the expanded image corresponds to 15 nm**

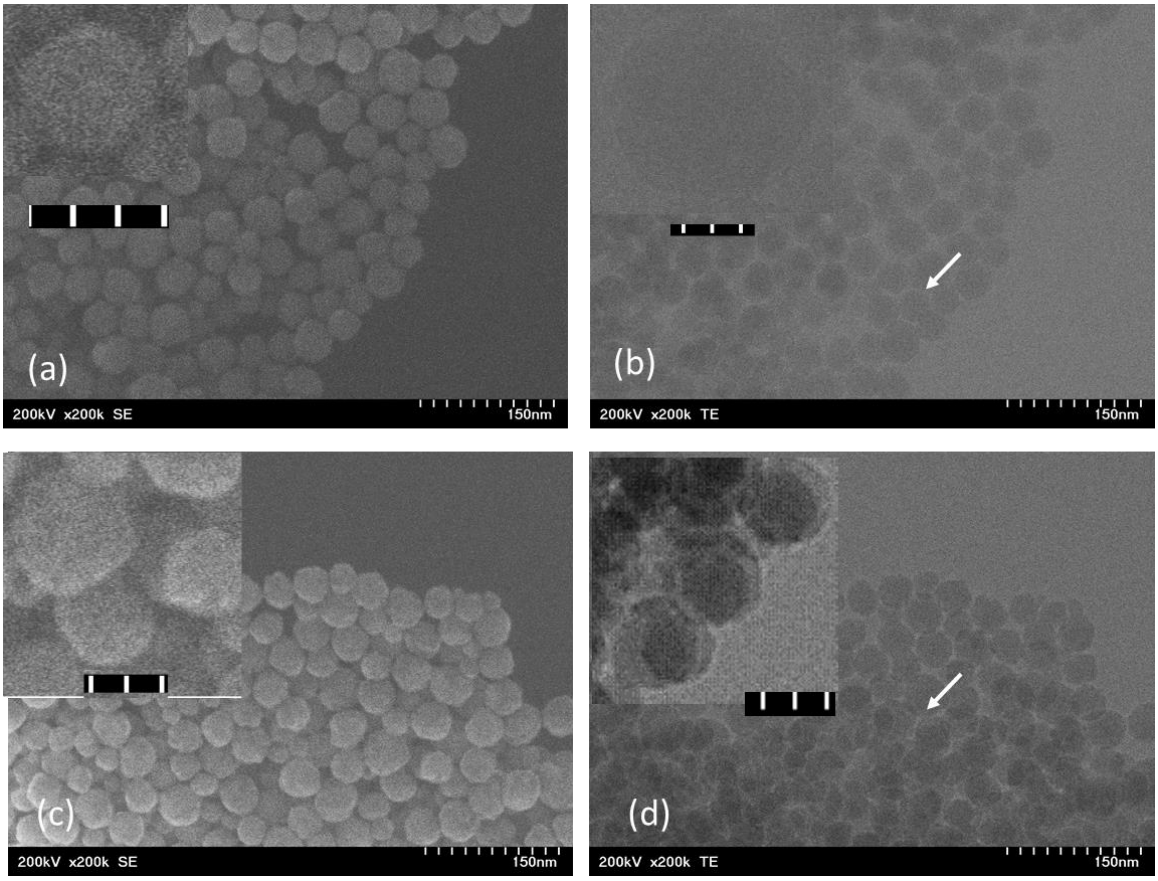


**Figure 5. Typical SEM (a) and STEM (b) images of colloidal particles from CS-50/ NIS and SEM (c) and STEM (d) images of those from PreEm-1. One scale of the dot bars in the inlets corresponds to 15 nm.**

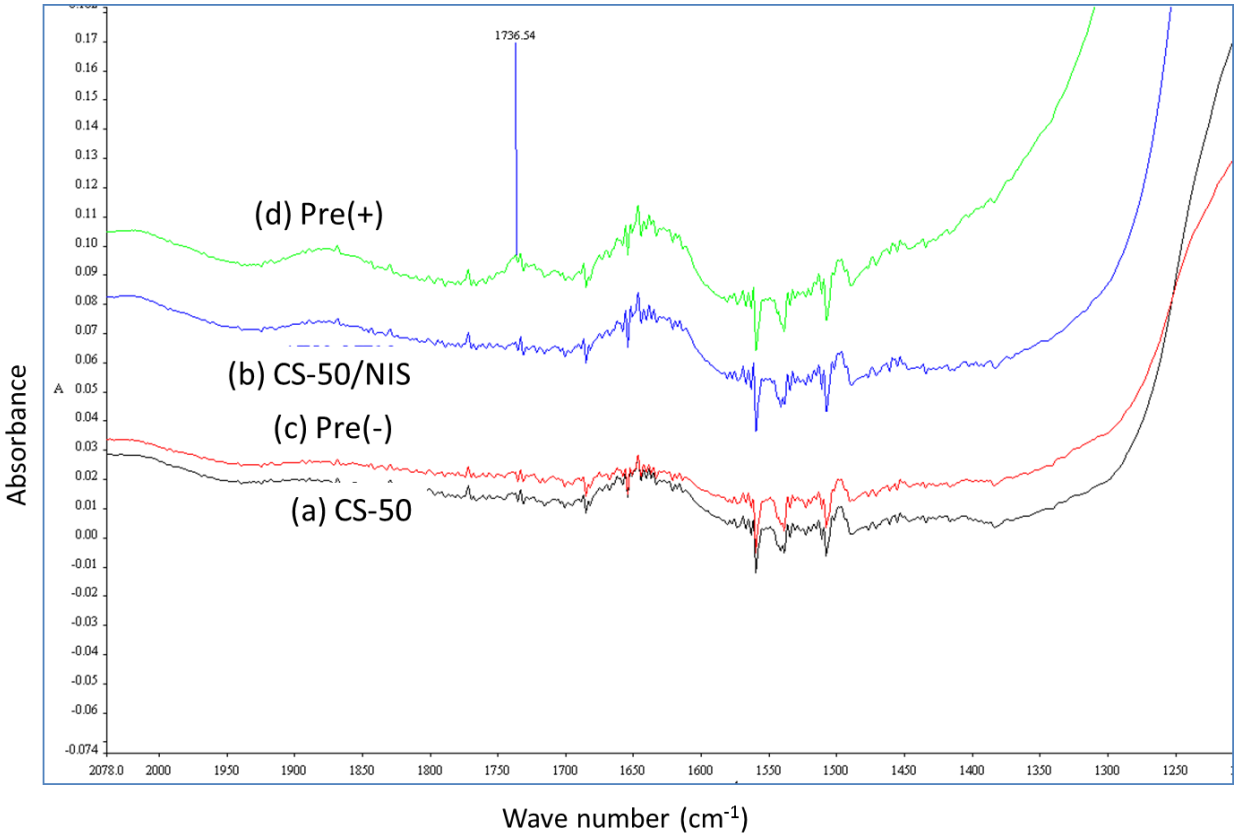


**Figure 6. Expanded IR spectra in the carbonyl stretching region of colloidal particles; (a) in the original CS-50, (b) after the NIS sedimentation, and in the pre-emulsion states prepared in the (c) absence and (d) presence of NIS.**

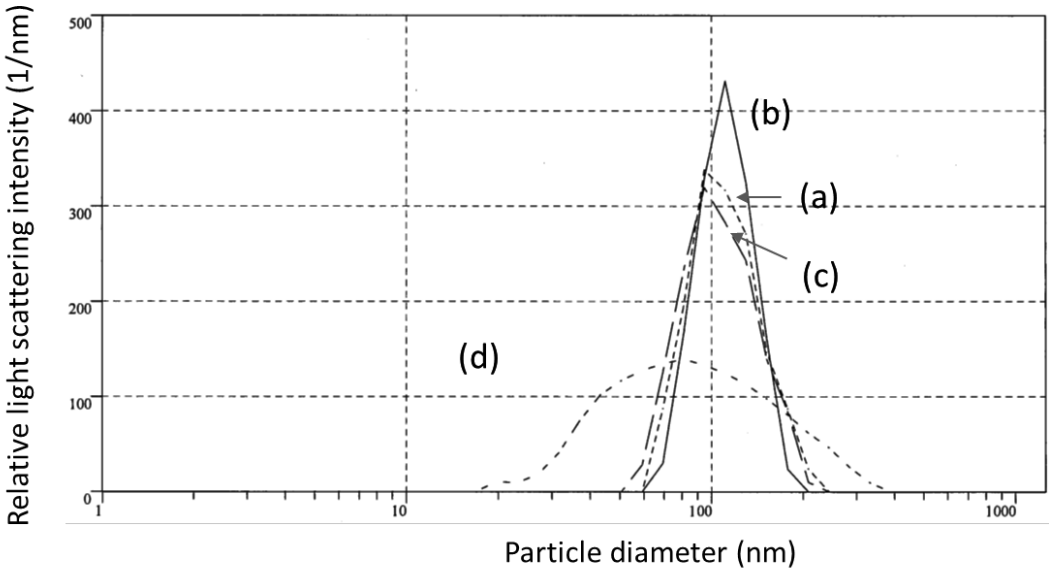


**Figure 7. Size distribution curves of the colloidal particles of (a) AcEm-1 (dotted line), (b) CS-50/ AcEm-1 (solid line), (c) PreEm-1/ AcEm-1 (dashed line), and (d) NCE-1 (dash-dotted line) as measured by DLS.**

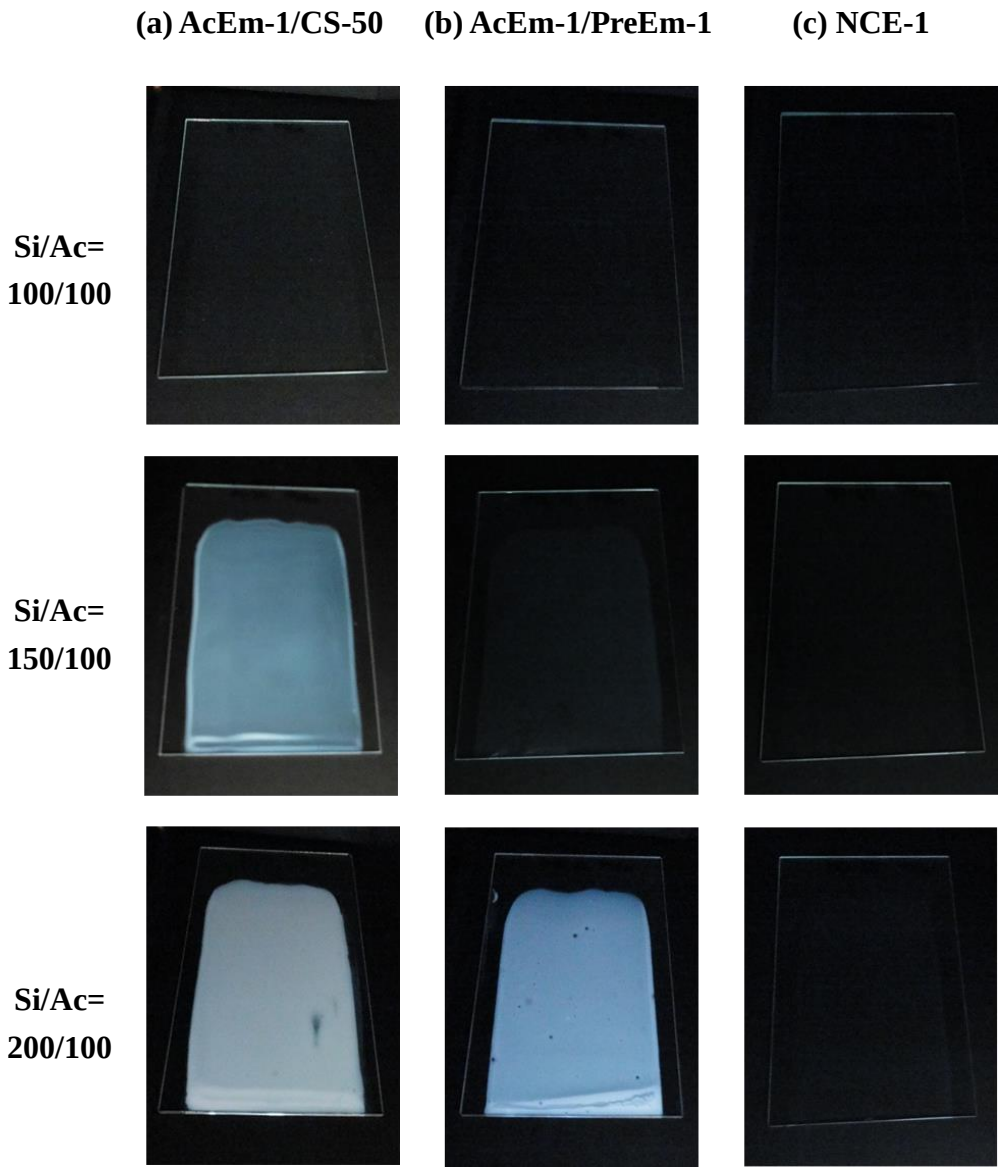


**Figure 8. Photos of the coating films of the three series of emulsions of (a) CS-50/ AcEm-1, (b) PreEm-1/ AcEm-1, and (c) NCE-1. The solid content was adjusted to 40 wt % with the Si/Ac ratios noted in the left side. The monomer composition of the polyacrylate was MMA/n-BA/MAA=34.5/65/0.5 in each series.**

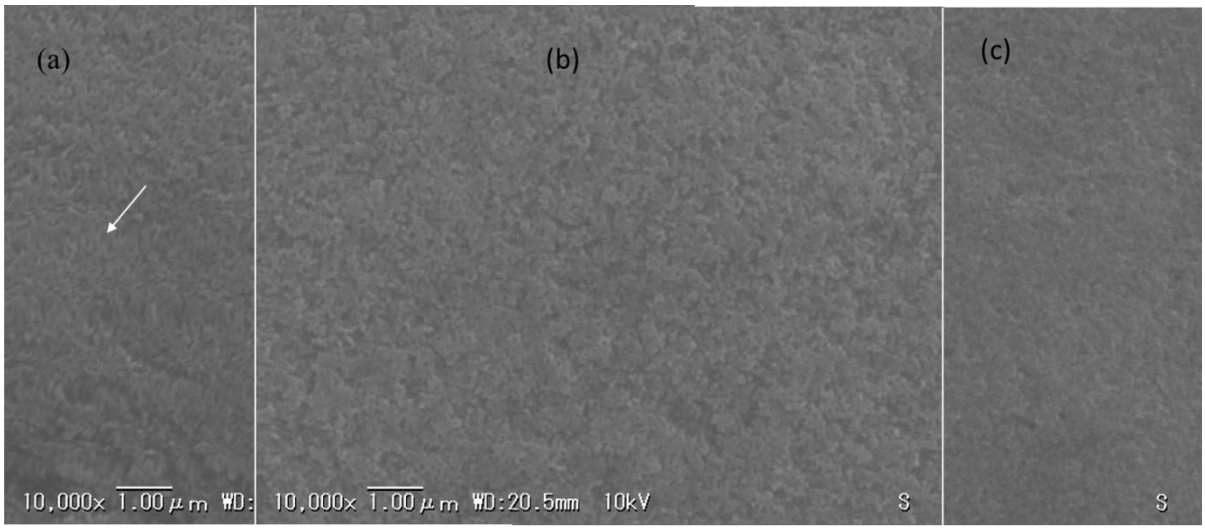


**Figure 9. SEM images of the cast films of the mixed emulsions of (a) CS-50/AcEm-1, (b) PreEm-1/ AcEm-1, and (c) NCE-1 (Si/Ac=150/100, MMA/n-BA/MAA=34.5/65/0.5).**

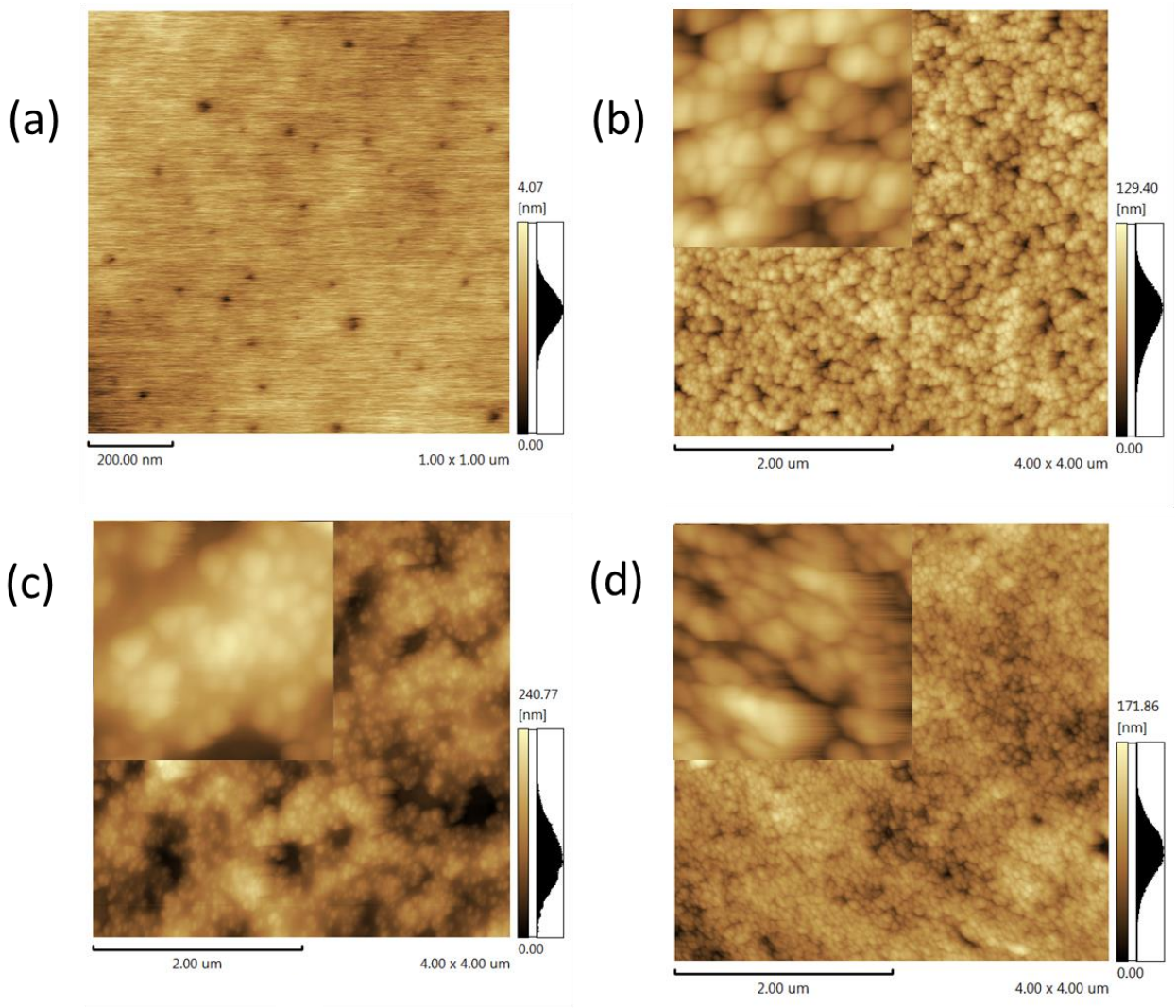


**Figure 10. AFM height images of the emulsions of (a) AcEm-1 (control), (b) CS-50/ AcEm-1, (c) PreEm-1/ AcEm-1, and (d) NCE-1 cast on a silicon wafer. The magnified images are shown in the inlets whose one side is 400 nm in length.**

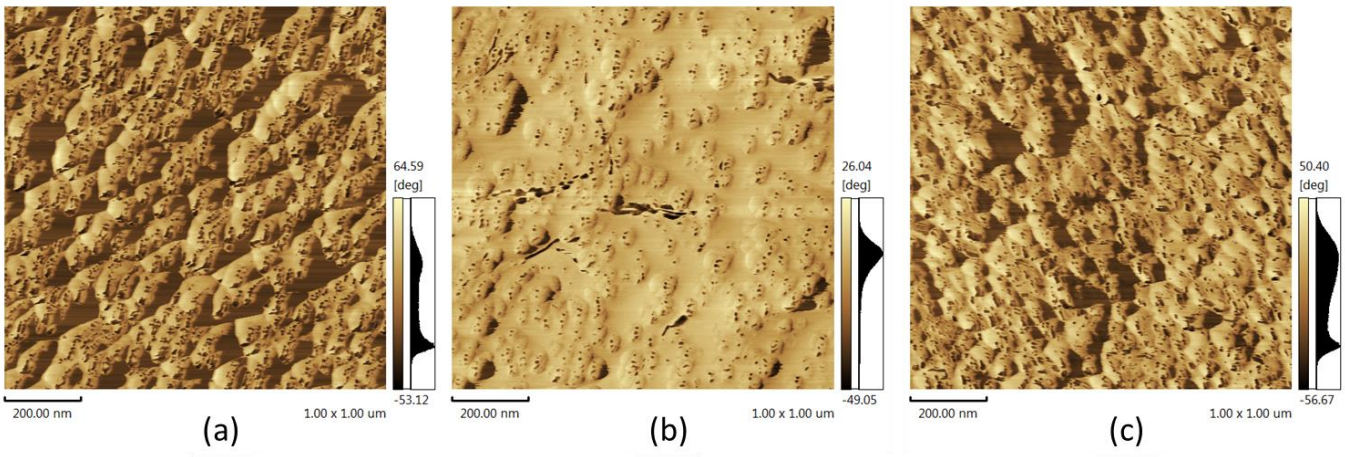


**Figure 11. AFM phase images of the emulsions of (a) CS-50/ AcEm-1, (b) PreEm-1/ AcEm-1, and (c) NCE-1 cast on a silicon wafer.**

(a) (b) (c)

**Figure 12. Photos of the coating films of the (a) CS-50/ AcEm-2, (b) PreEm-2/ AcEm-2, and (c) NCE-2 with Si/Ac= 150/100. The monomer composition of the polyacrylate of AcEm-2 was MMA/n-BA/MAA=53.3/46.3/0.4 (Tg= 10.0 ℃).**

## REFERENCES


1. M. Jianzhong, B. Yan, Z. Jing, *Adv, colloid and Interface Sci*., **197-198,** 118 (2013).
2. N. Dechao, Li. Yongsheng, S. Jianlin, *Chemical Society Reviews,* **46**, 569 (2017).
3. R. Tania, B. Carlos, F. Jose Paulo S., *Materials,* **7**, 3881 (2014).
4. K. Landfester, Angew. *Chem. Int. Ed.,* **48**, 4488 (2009).
5. J. Hu, M. Chen, L. Wu, *Polym. Chem.,* **2**, 760 (2011).
6. D. Qi, Z. Cao, U. Ziener, *Adv. Colloid Interf. Sci.,* **211**, 47 (2014).
7. M. Hood, M. Mari, R. Muñoz-Espí, *Materials*, **7**, 4057 (2014).
8. E. Bourgeat-Lami, GA. Farzi, L. David, JL. Putaux, TFL. McKenna, *Langmuir,* **28**, 6021 (2012).
9. K. Hamada, M. Kohri, T. Taniguchi, K. Kishikawa, *Colloid. Surf. A: Physicochem. Eng. Asp.*, **512**, 81 (2017).
10. LL. Hecht, T. Merkel, A. Schoth, C. Wagner, K. Köhler, R. Muñoz-Espí, K. Landfester, HP. Schuchmann, *Chem. Eng. J.*, **229**, 206 (2013).
11. T. Mizutani, K. Arai, M. Miyamoto, Y. Kimura, *J. Appl. Polym. Sci.,* **99**, 659 (2006).
12. T. Mizutani, K. Arai, M. Miyamoto, Y. Kimura, *Prog. Org. Coat.,* **55**, 276 (2006).
13. M. Yazdimamaghani, T. Pourvala, E. Motamedi, B. Fathi, D. Vashaee, L. Tayebi, *Materials*, **6**, 3727 (2013).
14. K. Arai, T. Mizutani, Y. Kimura, M. Miyamoto, *Prog. Org. Coat.*, **93,** 109 (2016).
15. M. Khalina, M. Sanei, HS. Mobarakeh, AR. Mahdavian, *Int. J. Adhes. Adhes.*, **58**, 21 (2015).
16. J. Ji, S. Shu, F. Wang, J. Liu, ZZ. Yu, *Colloid. Surf. A: Physicochem. Eng. Asp.*, **446**, 156 (2014).
17. E. Bourgeat-Lami, J. Lang, *J. Coll. Int. Sci.,* **210**, 281 (1999).

18. R. Hashemi-Nasab, SM. Mirabedini, *Prog. Org. Coat.,* **76**, 1016 (2013).

19. S. Song, S. Sun, H. Zhang, *Journal of Polymer Research,* **23**, 119 (2016).

20. ZB. Zhao, L. Tai, DM. Zhang, ZF. Wang, Y. Jiang, *Chem. Eng. J.,* **307**, 891 (2017).

21. H. Li, J. Yuan, H. Qian, L. Wu, *Prog. Org. Coat.,* **97**, 65-73 (2016).

22. Y. Wu, D. Hu, YH. Su, YL. Hsiao, B. You, L. Wu, *Prog. Org. Coat.,* **77** (6), 1015 (2014).

23. LL. Hecht, C. Wagner, Ö. Özcan, F .Eisenbart, K .Köhler, K .Landfester, HP. Schuchmann, *Macromol. Chem. Phys.*, **213**, 2165 (2013).

24. G. Canché-Escamilla, S. Duarte-Aranda, M. Toledano, *Mat. Sci. Eng. C.*, **42**, 161 (2014).

25. I. Sondi, TH. Fedynyshyn, R. Sinta, E. Matijevic, *Langmuir,* **16**, 9031 (2000).

26. MJ. Percy, SP. Armes, *Langmuir,* **18**, 4562 (2002).

27. MJ. Percy, C. Barthet, JC. Lobb, MA. Khan, SF. Lascelles, M. Vamvakaki. SP. Armes *Langmuir,* **16**, 6913 (2000).

28. D. Tumnantong, GL. Rempel, P. Prasassarakich, *European Polymer Journal,* **80**, 145 (2016).

29. E. Bourgeat-Lami, AJPG. França, TC. Chaparro, RD. Silva, PY. Dugas, GM. Alves, AM. Santos, *Macromolecules,* **49,** 4431 (2016).

30. XG. Qiao, O. Lambert, JC. Taveau, PY. Dugas, B. Charleux, M. Lansalot, E. Bourgeat-Lami, *Macromolecules,* **50**, 3796 (2017).

31. A. Khabibullin, E. Mastan, K. Matyjaszewski, S. Zhu, *Controlled Radical Polymerization at and from Solid Surfaces,* 29 (2015).

32. J. Ji, S. Shu, F. Wang, Z. Li, J. Liu, Y. Song, Y. Jia, *Nanoscale research letters*, **9**, 534 (2014)

33. X. Zhou, H. Shao, H. *Liu*, *Coll. Polym. Sci.,* **291**, 1181 (2013)

34. LL. Hecht, T. Merkel, A. Schoth, C. Wagner, K. Köhler, R. Muñoz-Espí, *Chem. Eng. J.* **229**, 206 (2013).

## LIST OF PUBLICATIONS

Chapter 1 “Unique structure and properties of inorganic-organic hybrid films prepared from acryl/silica nano-composite emulsions”

Koji Arai, Tsutomu Mizutani, Yoshiharu Kimura, Masatoshi Miyamoto

Progress in Organic Coatings, Vol. 93, pp. 109-117, 2016

Chapter 2 “Colloidal silica bearing thin polyacrylate coat: A facile inorganic modifier of acrylic emulsions for fabricating hybrid films with least aggregation of silicananoparticles”

Koji Arai, Tsutomu Mizutani, Masatoshi Miyamoto, Yoshiharu Kimura, Takashi Aoki

Progress in Organic Coatings, Vol. 128, pp. 11-20, 2019

## Other publications

"Development of a high-performance specialty paint, nano-composite emulsion, by inorganic-organic hybridization (an example for cooperative research among university, small industry, and government)"

Yoshiharu Kimura, Koji Arai, Tsutomu Mizutani

Journal of the Society of Fiber Science and Technology, Japan, Vol. 70, No. 6, pp. 180-183 (2014)

## Patents

"Aqueous coating composition and method for improving solvent resistance of coating"

Yoshiharu Kimura, Masatoshi Miyamoto, Tsutomu Mizutani, Koji Arai

Patent Appliation Laid-Open No. 352848/2004

"Organic-inorganic composite particle dispersion and method for producing"

Asami Kubo, Atsushi Takashima, Tomonori Hyodo, Tsutomu Mizutani, Koji Arai

Patent Appliation Laid-Open No.129737/2013

## Acknowledgment

The present investigation was carried out under the guidance of Late Professor Masatoshi Miyamoto at Department of Biomolecular Engineering, Kyoto Institute of Technology, Emeritus Professor Yoshiharu Kimura at Center for Fiber and Textile Science, Kyoto Institute Technology, and Associate Professor Takashi Aoki, Professor Hideki Yamane and Professor Shinichi Sakura at Department of Biobased Materials Science , Kyoto Institute of Technology in a period from 2013 to 2019. The author is deeply indebted to them for their constant guidance, encouragement, and valuable discussion throughout this work, and detailed criticism on the manuscript. The author is also very grateful to Dr. Tsutomu Mizutani at R&D Department of Mizutani Paint Co. Ltd for his kind assistance. Mizutani Paint Co. is highly acknowledged for providing the author with the opportunity of taking the PhD program in Kyoto Institute of Technology.

Finally, the author expressed his deep appreciation to his wife Mrs. Mai Arai and his family for their constant assistance and encouragement.

June, 2019

Koji Arai

Kyoto Institute of Technology